Cerebral Cortex, February 2018;28: 625–643

doi: 10.1093/cercor/bhw405
Advance Access Publication Date: 9 January 2017
Original Article

ORIGINAL ARTICLE

Axotomized Corticospinal Neurons Increase Supra-Lesional Innervation and Remain Crucial for Skilled Reaching after Bilateral Pyramidotomy

Alice C. Mosberger[1,2], Jenifer C. Miehlbradt[1,2], Nadja Bjelopoljak[1,2], Marc P. Schneider[1,2], Anna-Sophia Wahl[1,2], Benjamin V. Ineichen[1,2], Miriam Gullo[1,2] and Martin E. Schwab[1,2]

[1]Brain Research Institute, University of Zurich, Zurich, Switzerland and [2]Department of Health Science and Technology, ETH Zurich, Zurich, Switzerland

Address correspondence to Martin E. Schwab, Brain Research Institute, University of Zurich, Winterthurerstrasse 190, 8057 Zurich, Switzerland. Email: schwab@hifo.uzh.ch

Abstract

Skilled upper limb function heavily depends on the corticospinal tract. After bilateral lesions to this tract, motor control is disrupted but can be partially substituted by other motor systems to allow functional recovery. However, the remaining roles of motor cortex and especially of axotomized corticospinal neurons (CSNs) are not well understood. Using the single pellet retrieval task in adult rats, we induced significant recovery of skilled reaching after bilateral pyramidotomy by rehabilitative reaching training, and show that reach-related motor cortex activity, recorded in layer V, topographically reappeared shortly after axotomy. Using a chemogenetic neuronal silencing technique, we found that axotomized CSNs retained a crucial role for the recovered pellet retrieval success. The axotomized CSNs sprouted extensively in the red nucleus supplying new innervation to its magnocellular and parvocellular parts. Specific silencing of the rubrospinal tract (RST) also strongly abolished the recovered pellet retrieval success, suggesting a role of this cervically projecting nucleus in relaying cortical motor control. In summary, our results show that after bilateral corticospinal axotomy, motor cortex still actively engages in forelimb motor control and axotomized CSNs are crucially involved in the recovered reaching movement, potentially by relaying motor control via the RST.

Key words: electrophysiology, motor cortex, plasticity, reorganization, skilled reaching

Introduction

Impairment of upper limb function due to corticospinal tract (CST) lesions in spinal cord injury or stroke (Lang and Schieber 2003; Freund et al. 2012; Maraka et al. 2014) is a major cause of disability (Ma et al. 2014). Nonhuman primate (Lawrence and Kuypers 1968a; Hepp et al. 1974), feline (Pettersson et al. 2007), and rodent animal models (Weidner et al. 2001; Anderson et al. 2005; Friedli et al. 2015) have served to study this correlation of CST damage with impairments of upper limb motor skills, such as reaching and grasping behavior. Skilled reaching impairments have been shown to be most persistent when the lesion was placed in the brainstem (pyramidotomy), resulting in denervation of the whole cervical spinal cord and lower brainstem nuclei from direct cortical control (Whishaw et al. 1993; Weidner et al. 2001; Alstermark and Pettersson 2014). However, using the single pellet reaching task in rodents, which models human reaching and grasping movements (Whishaw et al. 1992a; Sacrey et al. 2009; Klein et al. 2012), it has been shown

that after unilateral pyramidotomy, rehabilitative training (Maier et al. 2008; Starkey et al. 2011), electrical stimulation (Brus-Ramer et al. 2007; Carmel et al. 2010, 2013), or molecular approaches (Thallmair et al. 1998; Cafferty and Strittmatter 2006; Liu et al. 2010) can lead to substantial compensatory sprouting of the intact CST into the denervated cervical hemicord and sprouting of corticobulbar fibers into brainstem nuclei. This form of plasticity allows the contralesional hemisphere to take over the function of the lesioned CST, leading to a high degree of functional recovery of skilled reaching (Ramic et al. 2006; Lindau et al. 2014; Wahl et al. 2014).

After complete bilateral pyramidotomy, however, all cortical motor commands must be relayed via other motor systems to regain functional recovery. Using plasticity-inducing therapies, sprouting of cortical projections above such a pyramidal lesion has been shown in the red nucleus, pons, and dorsal column nuclei (Thallmair et al. 1998; Z'Graggen et al. 1998). Furthermore, a recent study has shown a causal role of sprouting of unlesioned corticorubral neurons in skilled reaching recovery in rats after internal capsule stroke lesions (Ishida et al. 2016). These findings suggest a strong role of supra-lesional motor systems in functional recovery of skilled reaching, but the specific roles of motor cortex and of the axotomized corticospinal neurons (CSNs) themselves remain elusive.

Most recent studies on forelimb motor recovery after bilateral CST lesions have focused on the potential substitution of CST function by cervically projecting motor systems such as the rubrospinal tract (RST). Early experiments in nonhuman primates have reported some recovery of skilled upper limb movements after bilateral CST lesion which was disrupted by subsequent lesions of the RST (Lawrence and Kuypers 1968a, 1968b; Isa et al. 2013). In rodents, plasticity-inducing therapies have been shown to lead to extensive sprouting of rubral projections in the cervical spinal cord (Raineteau et al. 2001, 2002) as well as in different brainstem regions (Siegel et al. 2015) after bilateral pyramidotomy. A bilateral lesion of the RST in the cervical cord after recovery from a bilateral pyramidotomy led to an increased deficit in skilled reaching (Kanagal and Muir 2009). Similarly, in a mouse mutant entirely lacking a CST, rubrospinal innervation was increased and a strong forelimb motor deficit was induced by a cervical lesion of the RST (Han et al. 2015). Interestingly, red nucleus or RST lesions alone lead to only minimal impairments in skilled reaching tasks in primates and rats (Lawrence and Kuypers 1968b; Whishaw et al. 1998; Morris et al. 2011, 2015), suggesting a partial transfer of skilled upper limb function from the CST to the RST upon bilateral CST lesions across species. But it is unclear whether axotomized CSNs still contribute to skilled reaching recovery by relaying motor commands via this subcortical descending tract.

In the current study, we addressed this possibility by first investigating the remaining motor activity and role of the forelimb motor cortex in recovered reaching after bilateral pyramidotomy using chronic electrophysiological recordings and an ischemic stroke model. We then, through the use of specific neuronal silencing and anatomical tracing techniques, directly tested the role of the axotomized CSNs, as well as rubrospinal neurons (RSNs) in reaching performance after bilateral pyramidotomy.

To obtain a higher level of recovery of skilled reaching after bilateral pyramidotomy, we used intensive training of the single pellet retrieval task. Such training regimes have been shown previously to lead to rewiring of the intact CST after unilateral pyramidotomies (Maier et al. 2008, Starkey et al. 2011), and to increase recovery of reaching function (Weidner et al. 2001), potentially by reactivating the damaged circuitry and supporting the formation of functionally meaningful new connections (Starkey and Schwab 2012).

Materials and Methods

Subjects

A total of 121 adult female Long-Evans rats (Janvier, France), housed in groups of 3 to 4 per cage and kept on a 12:12 h light: dark cycle, were used. All but 18 animals, which were 20 weeks old, were 12 weeks old at the beginning of the experiment. Animals were fed ad libitum with standard rat chow and water when they were not used for behavioral training and for 5 days after any lesion. All behavioral experiments were performed in the light phase. During behavioral training, animals were kept on a limited diet of ~60% of the ad libitum food intake. A restricted amount of chow pellets was given directly after the training session. Animals that did not receive rehabilitative training (No Rehab group) received sugar pellets (45 mg Dustless Precision Pellets, Bio Serv) in their home cage. All animals were weighed on a regular basis to ensure no weight loss below 85% of ad libitum body weight. Experiments were approved by the Veterinary Office of the canton of Zurich, Switzerland.

Rehabilitative Training and Testing

Apparatus

All training and testing was performed using a custom-made skilled reaching setup. The Plexiglas box (15 × 40 × 30 cm) had a floor made of metal rungs (5 mm diameter, 8 mm spacing), a vertical window (1 cm wide, 5.5 cm high, starting 3 cm above the rungs) covered by a motorized door on one side, and a nose-poke sensor on the other side. Activating the nose-poke sensor opened the door covering the window. Outside of the window, a single sugar pellet was positioned on a pedestal (3 cm high, 14 mm in diameter, pellet 8 mm from box wall) for animals to retrieve with their forepaw. Door closure was performed manually after the pellet was retrieved or knocked off the pedestal.

Reaching Training

After a brief familiarization period, all animals were pretrained in the single pellet retrieval task for 12 days to reach baseline performance, performing 40 trials per daily session. The paw preference of animals was determined during the first sessions, upon which the pedestal was moved to the opposing side, allowing only reaches with this paw to target the pellet correctly. An additional 3–4 training days post-surgery were added for animals that received cervical and cortical virus injections. After bilateral pyramidotomy, animals in the Rehab group were further trained in skilled reaching as described above starting at 6 days post-lesion (dpl) and ending at 29 dpl, performing a total of 18 rehabilitative training sessions.

Reaching Testing and Analysis

Skilled reaching performance was tested on 3 days before lesion, and days 4, 5, 15, and 30 post-lesion. In each testing session, 20–25 reaching trials were performed and filmed to score success rates. Successful retrieval of the pellet from the pedestal on the first or after several attempts was scored 1 (first attempt success, *n*th attempt success). A trial in which the pellet was lifted from the pedestal but dropped inside or outside of the box was scored 0.5 (drop). If the pellet was knocked off the pedestal or the animal was incapable of reaching the pellet at

all, the trial was scored 0 (miss). Scores from all trials were summed and divided by number of total trials to calculate success score (percentage). The mean of the last 3 days before lesion was used as the baseline (bl) success score. No animals were excluded on the basis of their baseline performance. To evaluate the difference in the quality of recovery between Rehab (training induced) and No Rehab (spontaneous) animals, an additional analysis using only the non-missed trials was performed at the end of training (30 dpl). For this analysis animals that had missed trials only (0% success score) were excluded. The ratios of non-missed trials with outcomes first attempt success, *n*th attempt success, or drop, was then calculated for each animal and grouped into three performance levels (<1/3, >1/3 < 2/3, and > 2/3). The number of animals within each performance level was plotted for the 3 outcomes and the difference between Rehab and No Rehab group tested using a X^2 test (Fig. 1*E*).

Neuronal silencing was achieved by expression of hM4D receptors (DREADD, designer receptor exclusively activated by designer drug) (Urban and Roth 2015). Animals were tested before, and between 10 and 40 min after an i.p. injection of Clozapine-*N*-oxide (CNO, 1–2 mg/kg in 0.9% NaCl, Enzo Life Sciences), the inert ligand binding to hM4D, or 0.9% NaCl (saline control) performed under ~30–60 s isoflurane (5%) anesthesia. Scores obtained at 20–30 or 30–40 min after injection were used to assess performance under CNO and saline. Two animals of the Rehab group and four animals of the No Rehab group that received CSN silencing were additionally implanted with microwire arrays to perform chronic recordings from motor cortex (data not shown); these animals are represented as gray dots in Figure 5. Implantation of microwire arrays in these animals was performed between 15 and 30 dpl. No reduction in pellet retrieval success was found in these animals due to the array implantation (15 dpl: 17.5% ± 7.2%, 30 dpl: 26% ± 6.5%, $n = 6$, paired Student's *t*-test, $P = 0.22$, data not shown). Numbers of cells expressing hM4D in layer V of motor cortex (Fig. 5*C*) was not different when compared between animals with array implantations (1750 ± 234, $n = 6$) and without (1825 ± 180, $n = 23$) (unpaired Student's *t*-test, $P = 0.84$, data not shown), showing that the motor cortex was not significantly damaged due to implantations. Animals that had RSN silencing also received a forelimb motor cortex stroke at the end of the experiment and were tested again on days 2 and 3 after the stroke. Baseline performance for the stroke experiment was calculated from testing under saline, as this was performed shortly before the stroke lesion.

Surgical Procedures

General Procedures

All surgical procedures were performed under aseptic conditions. Anesthesia was induced by 5% isoflurane (Piramal Healthcare) in air and maintained by an i.m. injection of medetomidine (0.15 mg/kg Domitor, Orion Pharma), midazolanum (2 mg/kg, Dormicum, Roche), and fentanyl (5 μg/kg, Fentanyl 25, Kantonsapotheke) for lesions and stereotaxic injections, and an i.p. injection of ketamine (70 mg/kg Ketanarkon, Streuli) and xylazine (5 mg/kg Xylazin, Streuli) for procedures involving microstimulation. The skin was shaved and cleaned with ethanol and iodine (Betadine, Mundipharma), eyes were protected with a vitamin A containing eye ointment (Bausch & Lomb). During all surgeries, animals were kept on a heating pad. After surgery, all animals were injected s.c. with 5 mL saline/glucose (B. Braun), analgesic carprofen (5 mg/kg Rimadyl, Pfizer AG) and antibiotic enrofloxacin (5 mg/kg Baytril, Bayer). Medetomidine and midazolanum were reversed with atipamezol (0.75 mg/kg, Antisedan, Orion Pharma) and flumazenil (0.2 mg/kg, Anexate, Roche) s.c. Each animal was checked and weighed daily until 4 days after surgery and injected with Rimadyl and Baytril if they displayed signs of pain or stress.

Lesions

Bilateral pyramidotomies were adapted from previously reported studies (Maier et al. 2008; Starkey et al. 2011). Briefly, an incision was made between the chin and sternum and the connective tissue and muscles exposed with blunt dissection. Blunt forceps were used to pierce through the muscles to reach down to the ventral base of the skull. Muscle tissue was retracted with 4 hooks and the bone drilled open to expose the basilar artery and both pyramidal tracts. A micro-hook was used to remove the dura mater and dissect the pyramidal tract bilaterally. Muscle tissue and skin were sutured with stitches. Lesions were placed roughly between −11 and −13 mm caudal to Bregma at the level of the gigantocellular nucleus and inferior olives (Fig. 1*B*). All lesions were rostral to the ventral part of the medullary reticular formation (MdV).

Photothrombotic cortical stroke lesions in forelimb area were induced in animals that had received rehabilitative training after bilateral pyramidotomy (Lindau et al. 2014; Wahl et al. 2014). Briefly, animals were placed in a stereotaxic frame and skin above the skull was cut open with a scalpel and retracted with hooks. The bone was scraped dry and cauterized to ensure optimal penetration of light. A catheter was placed into the femoral vein and Rose Bengal (13 mg/kg, 10 mg/mL in 0.9% NaCl solution) was infused and the vein closed. An opaque template was placed on the skull with an open rectangle 4 mm lateral and 5 mm rostral from Bregma, on which a cold light source (Olympus KL 1500LCS, 150 W, 3000 K) was placed with a stereotaxic arm and the brain illuminated for 15 min. Subsequently, the skin was sutured.

Microstimulation

To ensure correct placement of microwire electrode arrays in forelimb motor cortex, microstimulation was performed as described previously (Lindau et al. 2014). Briefly, for intracortical stimulation, a glass isolated platinum/tungsten stimulation electrode (1–2 MΩ, Thomas Recordings) was used to deliver 50 ms trains of 0.2 ms biphasic pulses at 320 Hz and 80 μA. Before red nucleus injections, microstimulation was performed through the injection needle with the same pulse settings and 25–60 μA to ensure correct placement of rubral adeno-associated virus (AAV) injections. Forelimb motor cortex and red nucleus coordinates were inferred from stimulation induced forelimb movements detected by visual readout. The correct targeting of the red nucleus with the Cre-dependent AAV was further confirmed histologically using anatomical landmarks.

Stereotaxic Injections

To achieve specific expression of hM4D or eYFP from corticospinal and RSNs, a Cre expressing virus (AAV2.9_CaMKII.0.4.Cre.SV40, Penn Vector Core) was injected unilaterally into the cervical spinal cord. AAVs expressing hM4D or eYFP in a Cre-dependent manner were injected into forelimb motor cortex or red nucleus 2 days later. To ensure minimal impact on reaching performance, cervical injections were made in a least

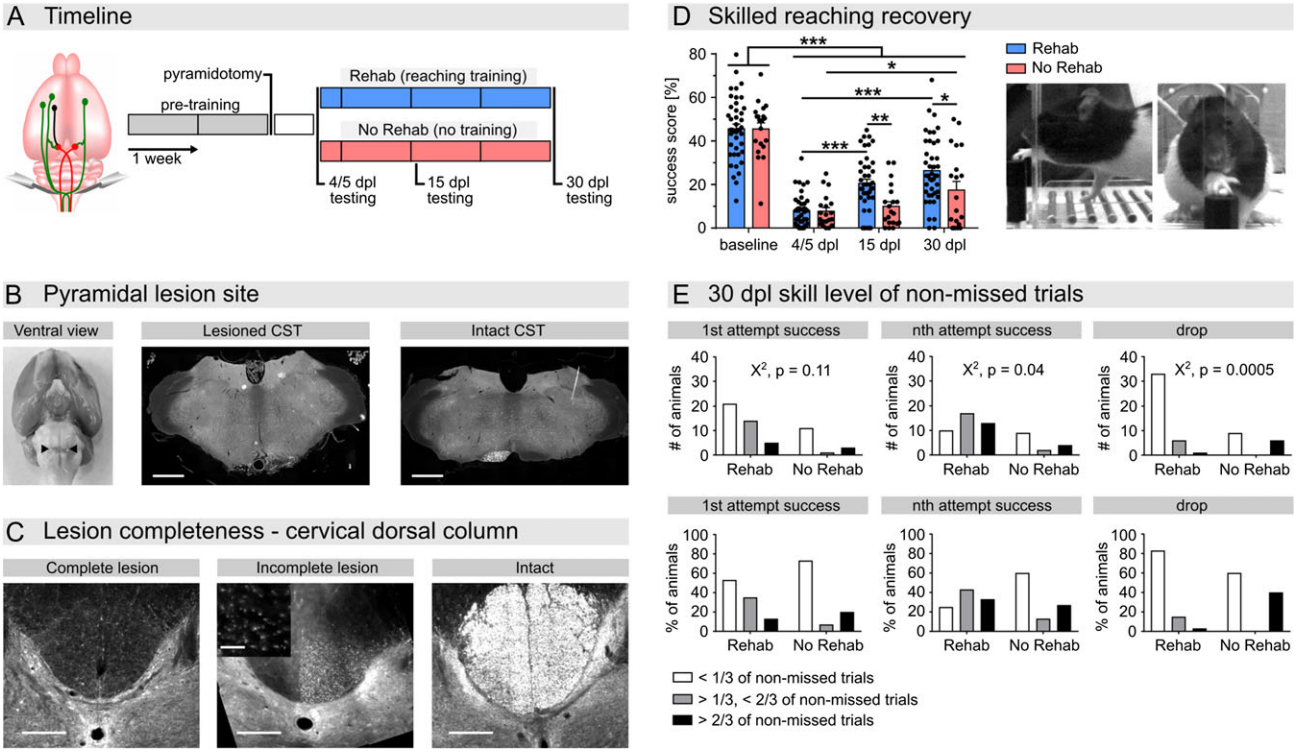

Figure 1. Recovery of skilled reaching after bilateral pyramidotomy. (*A*) Lesion design and experimental timeline. Animals received 2 weeks of pretraining in the single pellet retrieval task before a bilateral pyramidotomy was performed at the brainstem level. Post-lesion deficit in skilled reaching was assessed on days 4 and 5 post-lesion (dpl) and animals divided into 2 groups. Rehab animals (blue, $n = 42$) received daily training in skilled reaching until 30 dpl, while animals of the No Rehab group (red, $n = 20$) did not receive any training. Recovery of skilled reaching was assessed on 15 and 30 dpl. (*B*) Site of the bilateral pyramidal CST lesion. The bilateral lesion site in the brainstem (pyramidotomy) is indicated by the black arrowheads in the ventral view. Coronal sections at the level of the lesion show unilateral eYFP expression in corticospinal axons in an intact animal (Intact CST) and the bilaterally lesioned CST after pyramidotomy (Lesioned CST) (scale bar = 1000 μm). (*C*) Evaluation of lesion completeness. Fiber sparing was measured in the dorsal column of the cervical spinal cord by PKC-γ staining. The panels show a complete lesion with absence of the axonal CST marker PKC-γ in the dorsal column (Complete lesion), an incomplete lesion with partial axon sparing in the right dorsal CST (Incomplete lesion), and an intact animal (Intact) (scale bar = 100 μm). An inlet is shown with a close-up image of spared axons in the Incomplete lesion (scale bar = 10 μm). Animals with incomplete lesions were excluded from the study. (*D*) Skilled reaching assessed by the single pellet retrieval task requiring animals to reach through a narrow window with their forepaw for a sugar pellet on a pedestal. Before the lesion, both groups of animals had an average baseline success score of ~45% (Rehab: 45.5% ± 2.2%, No Rehab: 45.5% ± 2.8%). A bilateral pyramidotomy led to a strong impairment in skilled reaching success on 4 and 5 dpl (averaged Rehab: 8.0% ± 1.1%, No Rehab: 7.7% ± 1.6%, $P < 0.001$). Animals of the Rehab group recovered significantly already at 15 dpl (20.5% ± 2.0%, $P < 0.001$), and outperformed ($P < 0.01$) animals of the No Rehab group (10.0% ± 2.2%). At 30 dpl animals of the No Rehab group showed some recovery in skilled reaching (17.4% ± 4.0%, $P < 0.05$), but Rehab animals had significantly higher success scores (26.4% ± 2.3%, $P < 0.05$). Two-way ANOVA rep. measures, Bonferroni correction for multiple comparison. Data are represented as means + SEM, black dots represent single animals. (*E*) Skill level distribution on non-missed trials at the end of training. Absolute and relative number of animals within a certain skill level for the 3 possible outcomes of non-missed trials (first attempt success, *n*th attempt success, and drop). Rehab animals performed more *n*th attempt successes (X^2 test, $P < 0.05$) but had significantly less dropped attempts (X^2 test, $P < 0.001$). Rehab, $n = 40$; No Rehab, $n = 15$.

invasive way. A skin incision was made between the scapulae and the connective tissue removed by blunt dissection. A small incision was then made in the superficial muscle layer and deeper muscle layers were pulled apart with hooks. A laminectomy was performed on C4–C6 and the dura mater opened with microscissors. A total of 10 injection sites were targeted with a stereotaxic arm holding a 10 μL Nanofil Syringe with a 35 G needle controlled by an Ultra Micro Pump and a Micro 4 controller (World Precision Instruments). In each injection site 60 nL were injected at −1.0 and −1.2 mm from the surface of the spinal cord, respectively. Seven injection sites were distributed over the 3 segments at 1.0 mm lateral from the midline and an additional 3 injection sites at 0.6 mm lateral from the midline. All muscle layers and the skin were sutured at completion of surgeries. In 2 animals of the Rehab group and one animal of the No Rehab group that received CSN silencing AAV2.9_CaMKII.0.4.Cre.SV40 was injected into the CST lesion site (as described for Fast Blue in Supplementary Methods). These animals are represented as white dots in Fig. 5.

For injections into forelimb motor cortex, animals were placed into a stereotaxic frame and skin above the skull was cut open with a scalpel and retracted with hooks. The bone was scraped dry and cauterized at the coordinates of the craniotomy, which was made by drilling away the bone with a dental drill. Using the same pressure injection setup as for cervical injections, 6 stereotaxic injections were performed. Biotinylated dextran amine (BDA, 10 kD, Invitrogen) injections of 400 nL each were placed at AP/ML/DV 2.0/3.0/−1.0; 2.5/2.5/−1.0; 1.5/2.5/−1.0; 1.5/3.5/−1.0; 2.5/3.5/−1.0; 3.0/3.0/−1.0 mm from Bregma in the hemisphere contralateral to the animals reaching paw 4 weeks after the bilateral pyramidotomy. Injections of AAVs (AAV2.1_Ef1a_DIO_eYFP, AAV2.1_Ef1a_DIO_hM4D-mCherry, UNC Vector Core) were performed at the same coordinates using 200 nL each at 2 depths of −1.0 and −1.2 mm, 2 days after the cervical injections of the Cre expressing virus and before the bilateral pyramidotomy. Five animals from the Rehab group and 4 animals from the Intact group that received AAV2.1_Ef1a_DIO_eYFP additionally received AAV2.1_Ef1a_DIO_hM4D-mCherry at the same time, which did

not lead to mCherry expression but had no influence on eYFP intensity in the pyramidal tract. These animals are shown as white dots in Fig. 6.

To silence RSNs, a single injection of 50 nL of the AAV2.1_Ef1a_DIO_hM4D-mCherry into the red nucleus was performed accordingly using the following coordinates: AP/ML/DV −5.7/0.7/−6.0 mm from Bregma. In all animals, these coordinates were confirmed by electrophysiological microstimulation and visual readout of forelimb movements and slightly adjusted if necessary.

Microwire Electrode Array Implantation

Microwire electrode arrays (2 × 8 electrodes) were used in this study (Tucker-Davis Technologies). Electrodes were either 33 or 50 μm in diameter with an angled tip. Distance between electrodes within a row was either 350 or 500 μm with 500 μm row separation resulting in a recording area that spanned 2.45 × 0.5 mm or 3.5 × 0.5 mm, respectively in the caudal forelimb area. All animals were given Dexamethasone (1 mg/kg Mephameson, Mepha Pharma) one day before and on the day of surgery. Animals were anaesthetized as described above, placed in a stereotaxic frame and a craniotomy was placed above the forelimb motor cortex. The borders of the forelimb area were mapped by intracortical microstimulation as explained above. Three stainless steel bone screws (Fine Science Tools) were placed into the skull. The dura mater was removed and a piece of gel foam soaked in collagenase (20 mg/mL in 50 mM HEPES buffer containing 1 mM $CaCl_2$, Sigma-Aldrich) was placed on the surface of the brain to dissolve the pia mater (Kralik et al. 2001). After 3 min, the gel foam was removed and the craniotomy thoroughly washed with Ringer's solution (B.Braun). The microwire electrode array was placed on the surface of the brain and slowly moved into the brain so that the electrode tips came to lie −1.4 mm below the surface. Positioning of the electrode tips was confirmed by retrograde tracing of axotomized CSNs as described in Supplementary Methods. The ground wire was tightly wrapped around one of the bone screws and the reference wire was placed below the bone of the craniotomy. The craniotomy was then covered with Kwik-Sil (World Precision Instruments). Light curable dental cement (Tetric Evoflow, Ivoclar Vivadent) was used to cover the skull and fix the array in place. The skin was sealed with Histoacryl (B.Braun Medical). All animals were given antibiotics in their drinking water (Baytril, 2 mg/day, Provet) and were single housed for the duration of electrophysiological recordings.

Chronic Cortical Recordings and Electrophysiological Data Analysis

Reach-related activity was recorded on 3 days before pyramidotomy and on days 2, 4, 5, and 10 post-lesion as well as in unlesioned intact animals on the same days. To analyze reach-related multi-unit activity recorded in forelimb motor cortex, animals were filmed at 200 frames per second from a lateral view while performing the single pellet retrieval task (Dalsa Teledyne Camera). Activation of the nose-poke sensor was used as a digital trigger to time-lock the electrophysiological recordings to behavior. Frame by frame video analysis was performed extracting 2 events of each reaching trial: reach onset (lift-off of the paw from the rungs) and digit flexion (end of extension of the limb and flexion of the digits around the pellet). Earlier studies have shown persistent modulation of firing rates in forelimb motor cortex around these events during reaching movement (Dolbakyan et al. 1977; Hyland 1998). Electrophysiological signals were recorded at 25 or 32 kHz using a 16 channel USB-ME16 acquisition system (Multichannel Systems). Raw signals were band-pass filtered between 0.3 and 5 kHz using the MC_Rack software (Multichannel Systems) (see example trace Supplementary Fig. 1A). All further analysis was performed in Matlab (Mathworks), peri-event time histogramms (PETHs) were plotted with NeuroExplorer (Nex Technologies). To reduce artefacts, common average referencing was performed on all channels (Ludwig et al. 2009). Spikes were extracted using a threshold band of −3 to −6 standard deviations (SD) with a minimum of 1.5 ms of dead-time between spikes (see example waveforms Supplementary Fig. 1A). Furthermore, all extracted spikes that occurred in more than one channel at the same time were deleted from the dataset. Identification of reach-related multi-unit activity was performed as follows, leading to 4 classes of activity (Supplementary Fig. 1B,C). PETHs were calculated aligning spikes to reach onset and digit flexion events for each animal and channel using all trials of a recording session. Channels with less than 10 spikes per trial were classified as inactive (Supplementary Fig. 1B). For further analysis, spikes were combined into 20 ms bins and spike rate averaged over all trials of a session and over all bins of an interval. Baseline activity was calculated in the interval from −1.5 to −1 s before reach onset. Reach onset-related activity was calculated in the interval from −0.3 to +0.05 s around the onset event. Digit flexion-related activity from −0.2 to +0.05 s around digit flexion events. A channel was classified to be reach onset- or digit flexion-related if the activity around the respective event was higher than the baseline activity + (2 × SD) (Supplementary Fig. 1C). If a channel showed increased activity in both events, the class showing stronger activity was assigned. If a channel showed no increased activity around either reach event but was active overall, it was classified as unrelated (Supplementary Fig. 1B). Reach-related (onset- + flexion-related) and unrelated channels were counted for each animal and session. Positions of reach-related channels in the 2 × 8 electrode array were averaged for all animals of a group to generate cortical maps of activity (3D bar plots). Channel classifications were compared across recording days pre- and post-lesion and averaged for each group to investigate the stability and recovery of cortical activity.

Tissue Processing and Anatomical Analysis

Perfusion and Tissue Processing

Animals were perfused one week after BDA injection, or after all behavioral testing was completed, dependent on study. All animals were anaesthetized with 5% isoflurane, injected i.p. with 300 mg pentobarbital (Esconarkon, Streuli), and transcardially perfused with 200 mL Ringer's solution containing 100 000 IU/l heparin (Roche) and 0.25% $NaNO_2$ followed by 300 mL 4% paraformaldehyde (Sigma-Aldrich) 5% sucrose in 0.1 M PB, pH 7.4. Dissected brains were post-fixed in the same 4% formalin solution for 24 h and incubated in 30% sucrose in 0.2 M PB for 7 days at 4 °C. Brains and cervical spinal cords were frozen in blocks of Tissue-Tek O.C.T. (Sakura) and cryosectioned into 40 μm thick coronal sections on slide and stored at −20 °C.

Analysis of Lesion Completeness

Completeness of bilateral pyramidotomies was analyzed on coronal section of cervical spinal cord immunostained for protein kinase C-gamma (PKC-γ), a CST marker (Mori et al. 1990; Starkey et al. 2005). Sections were incubated overnight at room temperature with a rabbit anti-PKC-γ antibody (Santa Cruz Biotechnology, 1:200), which was detected with a goat

anti-rabbit Cy3 antibody (Molecular Probes, Intvitrogen, 1:300), incubated for 2 h at room temperature. The sections were then coverslipped in Mowiol (Calbiochem) and imaged with an Axioskop fluorescence microscope (Carl Zeiss). Stitched images of the dorsal column were acquired using a 20× objective. Two sections per animal were analyzed by placing 2 squared regions of interests (ROIs) of 900 μm^2 into the dorsal column of each section and counting remaining PKC-γ positive fibers with ImageJ CellCounter (NIH). Counts from the 4 ROIs were averaged for each animal. Animals with an average of more than 25 fibers per 900 μm^2 remaining were excluded from the study, ensuring motor complete lesions (Whishaw et al. 2003).

Analysis of Corticorubral Fiber Density

Innervation density in the red nucleus by all cortical projections was analyzed after anterograde tracing with BDA from the forelimb motor cortex. BDA positive fibers in the midbrain were visualized using a nickel-enhanced diaminobenzidine (DAB) staining as described previously (Maier et al. 2008). Briefly, endogenous peroxidase activity was quenched by incubating the sections in 50% EtOH and 0.3% H_2O_2 for 10 min. Sections were rinsed with TBST-X (50 mM Tris, 0.9% NaCl, 0.5% Triton X-100, pH 8.0) and incubated at 4 °C overnight with an avidin–biotin–peroxidase complex (Vectastain Elite ABC kit, Vector Laboratories). Then the sections were rinsed again in TBST-X and pre-incubated with 0.4% nickel ammonium sulfate (Sigma-Aldrich) in 0.05 M Tris, pH 8.0 for 10 min. Subsequently, 0.015% DAB (Sigma-Alrich) was added and sections incubated for another 10 min. The reaction was started by adding 0.004% H_2O_2 to the solution and was stopped in 0.05 M Tris after 5 min. After washing, sections were dried and dehydrated before being coverslipped in Eukitt (Kindler). Twelve sections, spanning the magno- and parvocellular parts of the red nucleus, were imaged with a slide scanner microscope (Mirax Midi Slide Scanner, Carl Zeiss).

Innervation of the red nucleus by purely corticospinal collaterals was analyzed using Cre-dependent eYFP expression in CSNs. Midbrain sections were stained with DAPI (1:40 000 in 0.05 M Tris, pH 8.0, Life Technologies) and coverslipped in Mowiol (Calbiochem). Twelve sections, spanning the magno- and parvocellular parts of the red nucleus, were imaged with a slide scanner microscope (Axio Scan.Z1, Carl Zeiss).

Fibers were counted in 8 bit images by measuring gray values along transversal parallel lines (at 25 μm distance) placed over the red nucleus (ImageJ) and peak detection (Matlab, Mathworks). Fiber counts were binned for 50 × 50 μm bins and summed along the rostro-caudal axis for 6 sections through the parvocellular and magnocellular parts of the red nucleus, respectively, according to the Rat Brain Atlas (Paxinos and Watson 2006). These summed projections were normalized for mean gray values (MGV) measured in the CST of the midbrain. Shortly, MGV was measured on 2 sections using a square of 150 × 150 μm and averaged for parvocellular and magnocellular red nucleus, respectively. These averages were then used to calculate a normalization factor (NF) for each animal by dividing its MGV by the study mean. The normalized fiber density was averaged for animals of each group to plot heat maps. Statistical analysis of fiber density was performed on ROIs of individual animals.

Reconstructions of hM4D-mCherry Expressing Neurons

hM4D-mCherry expressing neurons in forelimb motor cortex were counted on coronal sections. Sections were washed and coverslipped in Mowiol. Starting from the first rostral section with cortical neurons expressing mCherry, every fourth section was reconstructed and mCherry positive neurons counted and extrapolated for full volume using Neurolucida software (MBF Bioscience). To clearly separate hM4D-mCherry expression from auto-fluorescence of red nucleus neurons, midbrain sections were stained against mCherry by immunohistochemistry. Briefly, sections were first incubated in 50% EtOH and 0.3% H_2O_2 in water for 20 min and then in 0.1 M Tris containing 50 mM glycine for another 30 min. TNB/TBST-X (2:1) was used for permeabilization and blocking. Rabbit anti-mCherry antibody (1 mg/mL Abcam) was applied overnight at 4 °C 1:750 in blocking solution. After several washing steps, sections were incubated with biotinylated goat anti-rabbit antibody (1:300, Jackson Immuno Research) in TNB for 1 h at room temperature. Sections were further treated for DAB reaction as explained above; however, no nickel ammonium sulfate was applied. After coverslipping with Eukitt, every fourth section was reconstructed and mCherry positive neurons counted with the Neurolucida software, starting from the most rostral section with positive cells. Cell counts were extrapolated for the entire spanned volume.

Reconstructions of Stroke Volumes

To reconstruct the size of forelimb motor cortex stroke, sections were stained with NeuroTrace Fluorescent Nissl (1:500, Life Technologies) and coverslipped in Mowiol. Starting from the first rostral section with degenerated tissue, every sixth section was reconstructed, the stroke area outlined, and the volume calculated using the Neurolucida software.

Statistics

Statistical analysis was performed with Prism 7.0 (GraphPad Software Inc.). To detect differences between groups and within groups over time, two-way ANOVA with repeated measures followed by Bonferroni correction for multiple comparisons was used. For comparison of more than 2 groups or conditions, one-way ANOVA followed by Bonferroni correction for multiple comparisons was used. The Student's *t*-test was used to test for differences between 2 groups, or 2 time points within one group (paired). For comparisons of distributions, X^2 test was used. Two-tailed Pearson *r* was used to test for correlations. The threshold for significance for all experiments was set at $^{*}P \leq 0.05$. Smaller *P*-values were represented as $^{**}P \leq 0.01$ and $^{***}P \leq 0.001$. In bar graphs, all data are plotted as means + standard error of the mean (SEM) or absolute values. In box plot graphs, data are represented as median ± 25th percentile (box) and min/max (whiskers). Dots represent individual animals.

Results

Skilled Reaching Recovery after Pyramidotomy is Increased by Rehabilitative Training

Spontaneous and rehabilitative training-induced forelimb recovery after bilateral pyramidotomy was investigated with the single pellet retrieval task. As outlined in Fig. 1A, all animals were pretrained in reaching for single sugar pellets through a narrow window from a pedestal (40 trials/session) for 2 weeks to reach baseline performance, before receiving a bilateral lesion to the CST at the medullary level (Fig. 1B). At 4 and 5 dpl, the lesion deficit was assessed and animals were randomly split into a Rehab and a No Rehab group with equal mean and variance.

Rehab animals received daily skilled reaching training, while No Rehab animals did not receive any training. All animals were tested for recovery at 15 and 30 dpl. Lesion completeness was assessed by PKC-γ staining of the cervical spinal cord (Fig. 1C). Animals with incomplete lesions were excluded from the study ($n = 10$). Figure 1D shows the pellet retrieval success rate combining all animals used for rehabilitative training (Rehab) or no training (No Rehab), except for animals used for chronic electrophysiological recordings. By using a pedestal to place the pellet and scoring dropped pellets only with 0.5 points, we measured a baseline performance of ~45% success rate in both groups. This performance is in line with previous results using pedestals (Buitrago et al. 2004). Both groups showed a significant lesion impairment compared with baseline scores ($P < 0.001$) with an initial reduction of performance to ~8% at 4/5 dpl (averaged). Animals of the Rehab group already recovered substantially to ~20% only 10 days later at 15 dpl ($P < 0.001$), showing a significantly higher success score than No Rehab animals (~10%, $P < 0.01$). By 30 dpl, No Rehab animals showed some spontaneous recovery of pellet retrieval success compared with 4/5 dpl ($P < 0.05$), performing at ~17% success rate. However, animals receiving rehabilitative training outperformed the No Rehab group significantly (~26%, $P < 0.05$). This result suggests that the intensive retraining of the skilled reaching movement after bilateral pyramidotomy allowed functional recovery of reaching. To evaluate whether the rehabilitative training resulted in skilled movement recovery at 30 dpl that was fundamentally different than the spontaneous recovery seen in No Rehab animals, we further analyzed the performance of animals on trials in which the pellet was not missed. Figure 1E shows the distribution of animals with low (<1/3 of non-missed trials), medium (>1/3, <2/3 of non-missed trials), or high (>2/3 of non-missed trials) skill level for both groups and for each of the possible non-missed trial outcomes. X^2 testing revealed a significantly different distribution for Rehab and No Rehab animals for nth attempt success ($P < 0.05$) and drop trials ($P < 0.001$). Thus, rehabilitative reaching training led to an increased reaching skill level than resulted from spontaneous recovery. We next investigated whether forelimb motor cortex played a crucial role in such recovered skilled reaching performance.

Forelimb Motor Cortex Stroke Abrogates Recovered Pellet Reaching after Pyramidotomy and Rehabilitation

To investigate the role of forelimb motor cortex in recovery of skilled reaching after pyramidotomy, animals of the Rehab group received a lesion to the forelimb motor cortex after 30 dpl (Fig. 2A). Using the photothrombotic method, a stroke was induced in the contralateral hemisphere relative to the reaching paw leading to a cortical lesion comprising ~19% of the hemisphere volume anterior to Bregma and thus the entire caudal and rostral forelimb area (Fig. 2B). This forelimb motor cortex stroke led to a significant drop in skilled reaching success rate 2/3 days post-stroke compared with pre-stroke scores ($P < 0.05$, Fig. 2C) with the majority of animals showing a strongly reduced success rate. To evaluate if the change in success rate was due to a loss of targeting skill or an increase in dropped attempts, the ratio of each non-missed trial outcome was plotted before and after stroke. However, analysis of this performance profile (Fig. 2C) failed to show a significant difference for either of the trial types and no definite cause for the overall reduction in pellet retrieval success can be assigned. To further investigate the role of motor cortex in reaching after bilateral pyramidotomy, we next performed electrophysiological recordings from motor cortex to ask whether movement-related activity in cortical circuitry occurred with recovered skilled reaching movements.

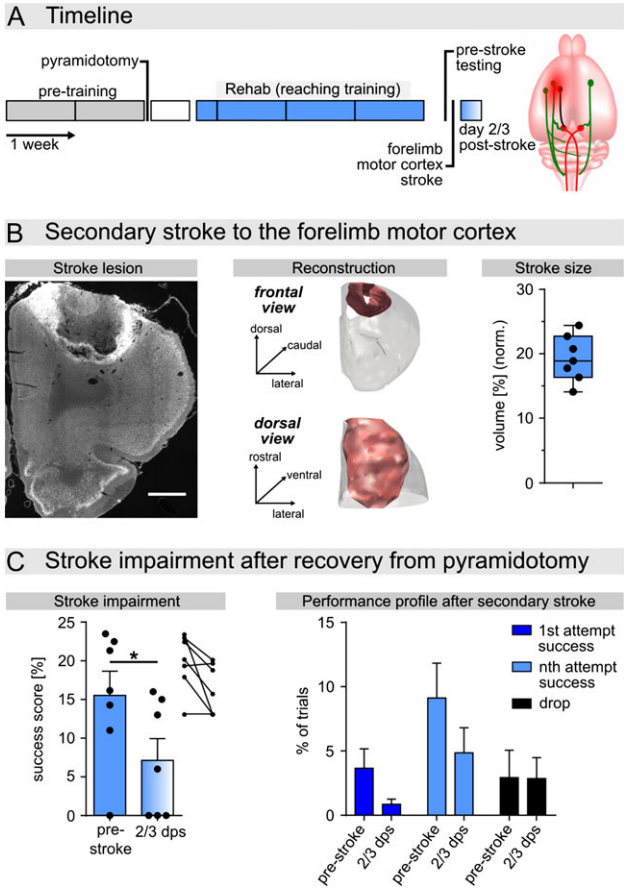

Figure 2. Impairment in recovered skilled reaching performance after forelimb motor cortex stroke. (A) Experimental timeline and lesion design. Animals that had received a bilateral pyramidotomy and rehabilitative training ($n = 7$) were tested for skilled reaching recovery and subsequently received a forelimb motor cortex stroke to the contralateral hemisphere of the reaching paw. The post-stroke deficit was measured on days 2 and 3 post-stroke and averaged. (B) Stroke lesion shown on a coronal section counterstained with NeuroTrace (scale bar = 500 μm). The degenerated tissue covers all cortical layers. A representative reconstruction of the stroke volume (pink) is shown in a frontal (top) and a dorsal view (bottom). Stroke size was normalized to the whole hemisphere anterior to Bregma and comprised 19.3% ± 1.4% of the volume. (C) Skilled reaching score after forelimb motor cortex stroke showed a significant mean deficit (pre-stroke: 15.5% ± 3.1%, 2/3 dps: 7.1% ± 2.8%, paired Student's t-test, $P < 0.05$, $n = 7$). The inlet shows performance of single animals connected with lines. The performance profile showing ratio of trials with first and nth attempt success or drops did not show a significant difference for pre- and post-stroke measurements (Two-way ANOVA rep. measures, time: $P = 0.089$). Box plot data are represented as median ± 25th percentile (box) and min/max (whiskers). Bar graph data are represented as means + SEM. Black dots represent single animals.

Reach-Related Cortical Activity Reappears in Rats with Pyramidotomy and Rehabilitative Training

To investigate whether rehabilitative training engages prelesional cortical reaching circuitry, activity in the caudal forelimb area of motor cortex was recorded before and after bilateral pyramidotomy (Fig. 3). Animals were pretrained in skilled reaching for 2 weeks and implanted with 2 × 8 microwire electrode arrays into forelimb motor cortex layer V contralateral to the

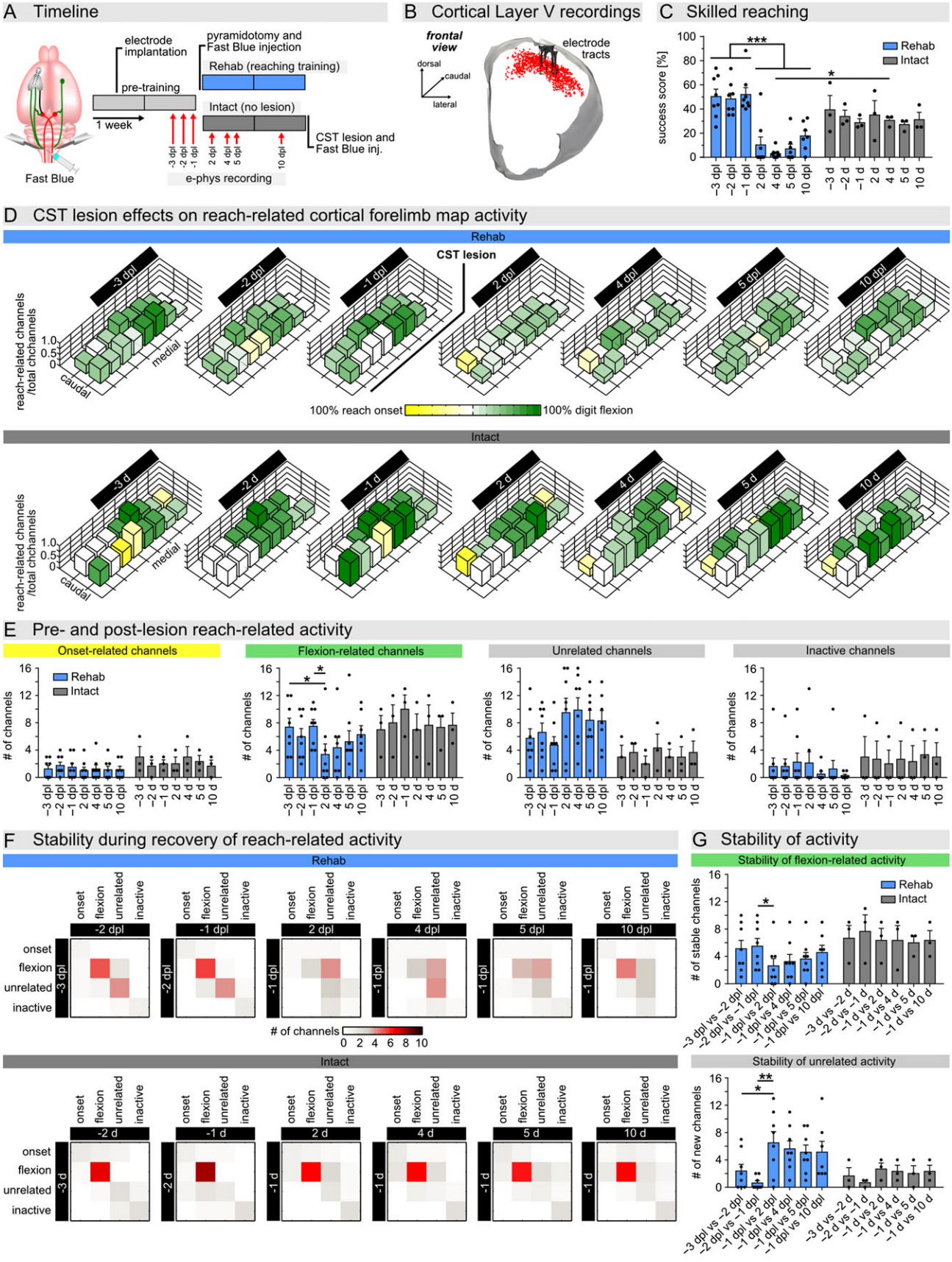

Figure 3. Reach-related motor cortical activity after bilateral pyramidotomy. (A) Experimental design and timeline. Animals were pretrained in skilled reaching for 2 weeks during which they were implanted with a 2 × 8 microwire electrode array into the forelimb motor cortex contralateral to the reaching paw. Multi-unit activity

reaching paw. Multi-unit activity was analyzed on 3 days prior to pyramidotomy and on days 2, 4, 5, and 10 after lesion (Rehab) and on corresponding days in an unlesioned group (Intact) (Fig. 3A). One animal of the Rehab group lost its headmount after 5 dpl and was not recorded at 10 dpl (Animal #8, Supplementary Fig. 1D). Placement of electrodes in cortical layer V was confirmed by reconstruction of retrogradely labeled CST neurons and electrode tracts (Fig. 3B). Electrode implantation or recording during skilled reaching training did not disrupt the behavior of the animals or the reaching score, which stayed stable for Intact animals (~32%) and for Rehab animals before lesion (~50%). Reaching performance was significantly impaired in Rehab animals after lesion ($P < 0.001$) with lowest scores at 4 dpl and a partial recovery to ~18% at 10 dpl (Fig. 3C). Two specific kinematic events in skilled reaching movement were used to detect reach-related activity in forelimb motor cortex: reach onset = lift-off of the limb (yellow in Fig. 3D,E and Supplementary Fig. 1), and digit flexion = start of paw closure around the pellet (green in Fig. 3D,E,G and Supplementary Fig. 1). Supplementary Fig. 1C shows both reach events and representative PETHs for reach-related channels. Reach-related channels were topographically arranged in forelimb motor cortex across animals as shown in Fig. 3D. Electrode positions in the caudal part of the array had a higher percentage of reach onset-related activity (yellow), while rostral areas were mainly digit flexion-related (green) in Intact and Rehab groups. This averaged topography seemed stable over time. The height of bars in Fig. 3D indicates the average ratio of combined reach-related channels/total channels for each group. Early after pyramidotomy, the Rehab group showed a reduction of reach-related channels over the whole map (reduced bar height) with a main loss of flexion-related activity (green). However, over the following post-lesion recording days, the pre-lesion activity pattern reappeared. A quantification of all channel classifications over time showed that the pyramidotomy had the strongest impact on digit flexion-related channels which were strongly reduced at 2 dpl ($P < 0.05$, Fig. 3E). This reduction in flexion-related channels partially recovered over the post-lesion period. The total number of unrelated channels showed a slight but insignificant increase after the lesion, while reach-onset and inactive channel counts were unchanged (Fig. 3E). These findings suggest that pyramidotomy only had a transient effect on mainly flexion-related cortical activity.

To investigate whether pyramidotomy and reaching recovery affected stability of cortical activity, we next compared channel classifications across days. All 16 channels from each animal were classified as onset-related, flexion-related, unrelated, or inactive as described above, and classifications compared across pre-lesion days and between −1 dpl and post-lesion days. This post-lesion comparison was performed to investigate whether reappearance of flexion-related activity occurred in the same channels that showed this activity before the lesion. Figure 3F shows heat maps indicating the average number of stable and switching channels for each class. In both groups, most channels showed stable classification when compared across unlesioned days, with the highest number of channels showing stable flexion-related activity. The pyramidotomy initially led many flexion-related channels to become unrelated. But the original flexion-related channels reappeared over time (Fig. 3F, −1 dpl vs. 2 dpl and −1 dpl vs. 10 dpl). To quantify these dynamics, the number of stable flexion-related channels was counted on the same day comparisons (Fig. 3G). Pyramidotomy led to an initial reduction in stable flexion-related channels on 2 dpl ($P < 0.05$), which recovered over time, further corroborating that flexion-related activity reappeared in previous cortical areas. Pyramidotomy also led to a strong increase in newly classified unrelated channels at 2 dpl (Fig. 3G; $P < 0.01$, $P < 0.05$), which showed some tendency to recover over time. Taken together, these results suggest that cortical reach-related activity is disrupted shortly after pyramidotomy, but reappears to mimic the pre-lesion state. Classification of all channels for each animal across all days is shown in Supplementary Fig. 1D, providing further qualitative proof of this finding. Thus, rehabilitative reaching training likely activates cortical reaching circuits in a similar manner as reaching training in the intact condition. The activation of these stable cortical networks could induce anatomical rerouting toward subcortical motor areas allowing relay of motor commands. To investigate this possibility, we have focused our analysis on one potential target for such anatomical reorganization, the red nucleus.

Total Corticorubral Innervation is Only Mildly Affected by Rehabilitative Training

The red nucleus is generally separated into a caudal magnocellular and a rostral parvocellular part, while the magnocellular

was recorded on 3 days prior to the pyramidotomy and on days 2, 4, 5, and 10 after the lesion (Rehab, blue, $n = 8$, 10 dpl $n = 7$); and on corresponding days in a second, Intact, group (gray, $n = 3$). Intact animals received a pyramidotomy at the end of the experiment. To confirm electrode placement, Fast Blue was injected into the lesion site to label axotomized CSNs. (*B*) Reconstruction of a hemisphere with Fast Blue positive cells (red) in the forelimb motor cortex and electrode tracts (black) of the microwire array. (*C*) Skilled reaching success scores. Pyramidotomy led to a strong deficit in skilled reaching performance (pre-lesion: 50.2% ± 4.8%, 4/5 dpl: 5.0% ± 2.3%, $P < 0.001$), which was significantly reduced compared with intact animals on 4 dpl (Rehab: 3.0% ± 1.4%, Intact: 30.6% ± 2.8%, $P < 0.05$). Intact animals showed stable reaching success over the recording period with success rates ~32.2% ± 5.2%. (*D*) Cortical maps of reach-related channels. Projection of the 2 × 8 electrodes in the forelimb motor cortex averaged over all animals showing areas of reach onset- (yellow) or digit flexion- (green) related activity for each recording day split by group. The height of the bars show the ratio of reach-related channels/total channels. Pyramidotomy reduced the overall number of reach-related channels with a decrease of digit flexion-related activity. The topography of the cortical map reappeared at 5 and 10 dpl. (*E*) Quantification of reach-related, unrelated, and inactive channels pre- and post-lesion. The average number of reach onset-related channels was stable over time in Rehab (~1.3 ± 0.5) and Intact animals (~2.2 ± 1.0). The average number of digit flexion-related channels dropped significantly after the lesion (−3 dpl: 7.4 ± 1.3, vs. 2 dpl: 3.4 ± 1.6, $P < 0.05$; −1 dpl: 7.5 ± 1.0, vs. 2 dpl, $P < 0.05$), and recovered over the post-lesion period (10 dpl: 6.3 ± 1.3) in Rehab animals, but was stable over time in Intact animals (~7.9 ± 2.2). The number of unrelated channels increased slightly after the pyramidotomy in Rehab animals (pre-lesion: ~5.7 ± 1.3, post-lesion: ~9.0 ± 1.7), and was unchanged in Intact animals (~3.2 ± 1.5). Inactive channels were low in most animals over the whole course of the experiment (Rehab: ~1.4 ± 1.0, Intact: ~2.7 ± 2.4). (*F*) Average channel classifications across days showing pre-lesion stability and post-lesion recovery. Compared pre-lesion days and all Intact animal comparisons show high stability of channel classification over time, with most channels being and staying flexion-related. Pyramidotomy led to a transient shift of flexion-related channels to become unrelated (−1 dpl vs. 2 dpl, Rehab). This shift steadily recovered over time and the same pre-lesion flexion-related channels reappeared (−1 dpl vs. 10 dpl). (*G*) Quantification of stability of activity. The number of stable flexion-related channels across days was significantly reduced only early after pyramidotomy (−2 dpl vs. −1 dpl: 5.5 ± 1.1, −1 dpl vs. 2 dpl: 2.6 ± 1.1, $P < 0.05$). Intact animals showed no change in stable flexion-related channels over time (~6.6 ± 1.8). Pyramidotomy led to an increase in the appearance of new unrelated channels (−3 dpl vs. −2 dpl: 2.4 ± 1.0, −1 dpl vs. 2 dpl: 6.5 ± 1.6, $P < 0.05$; −2 dpl vs. −1 dpl: 0.6 ± 0.3, −1 dpl vs. 2 dpl: 6.5 ± 1.6, $P < 0.01$), which was stable in Intact animals (~1.9 ± 0.9). Two-way ANOVA rep. measures, Bonferroni correction for multiple comparison. Data are represented as means + SEM, black dots represent single animals.

part is known to project to the spinal cord forming the RST (Gwyn and Flumerfelt 1974; Kennedy 1990). However, in rodents, both parvocellular and magnocellular parts give rise to the RST in a topographic organization along the rostro-caudal axis (Brown 1974a, 1974b; Liang et al. 2012) and the parvocellular part receives stronger cortical input. To investigate the density of corticorubral innervation, animals of the Rehab and No Rehab groups were injected with anterograde axonal tracer BDA into the forelimb motor cortex after 30 dpl (Fig. 4A) and perfused one week later. Intact animals were also traced with BDA. A fourth group of animals (Acute lesion) was injected with BDA and received a bilateral pyramidotomy 5 days later to control for axotomy effects on staining intensity. Fibers innervating the parvocellular and magnocellular parts of the red nucleus were counted on coronal sections (Fig. 4B). Lateral, ventral, and medial regions of the cup-shaped innervation area (ROIs) were selected on coronal projection plots and analyzed for fiber density (Fig. 4C,E). Fiber density in the parvocellular red nucleus did not show any difference between the groups for either ROI when normalized to staining intensity in the pyramidal tract (Fig. 4D). Innervation of the magnocellular red nucleus was slightly increased on group average level for animals of the Rehab group (Fig. 4E); however, analysis of fiber density in individual ROIs did not show a significant difference between groups (Fig. 4F). These findings suggest that corticorubral bulk innervation was not changed by the pyramidotomy or rehabilitative reaching training. We next investigated whether the axotomized CSNs were involved in mediating recovered reaching skill.

Axotomized CSNs Mediate Recovery of Skilled Reaching after Pyramidotomy

CSNs have been shown to survive several weeks after axotomy in the pyramids in mice, but undergo synaptic loss (Ghosh et al. 2012). Using retrograde tracing with Fast Blue injected into the lesion site, we quantified numbers of CSNs in the motor cortex 1 and 5 weeks after lesion. No difference was found in surviving CSN numbers (Supplementary Fig. 2), allowing axotomized CSNs to potentially reconnect above the lesion and mediate behavioral control. To investigate the role of CSNs in recovery of skilled reaching, a silencing DREADD construct (hM4D) (Urban and Roth 2015) was expressed specifically in the axotomized CSNs using a Cre-dependent double AAV transfection approach in Intact animals and animals about to receive a bilateral pyramidotomy (Rehab and No Rehab groups). After 30 dpl, animals were tested during CSN silencing by the hM4D ligand CNO and under saline (Fig. 5A). HM4D.mCherry was strongly expressed by CSNs in the forelimb motor cortex at the end of the experiment (Fig. 5B). Figure 5C shows the extrapolated cell numbers for all groups being similar for Rehab and No Rehab groups (~1900), with insignificantly fewer cells in Intact animals (~1350). Bilateral pyramidotomy led to a strong behavioral deficit with low post-lesion success scores of ~6% in both Rehab and No Rehab groups ($P < 0.001$), while only the Rehab group showed recovery of skilled reaching at 15 dpl ($P < 0.05$) and 30 dpl ($P < 0.001$) to ~20% success score (Fig. 5D). When tested after i.p. injection of CNO, the Rehab animals showed a significant impairment from ~19% to ~12% success score ($P < 0.05$), which was not found after saline injection or in No Rehab or Intact animals (Fig. 5E). Considering that the lesion to the entire forelimb motor cortex led to a similar drop in performance (~8%) (Fig. 2B), this finding indicates that, among cortical projection neurons, CSNs play a central role in recovery of skilled reaching after bilateral pyramidotomy. Furthermore, analysis of the ratios of trials with non-missed outcomes (performance profile) of Rehab animals shows that CSN silencing specifically reduced the first attempt success rate ($P < 0.05$), while *n*th attempt successes and drops were unchanged (Fig. 5F). These data indicate that CSN silencing specifically impaired the precise targeting of the pellet, while the skill of bringing the pellet securely to the mouth was not affected. Reaching performance of the No Rehab group showed only minor spontaneous recovery which did not allow the detection of a CSN silencing-induced deficit (Fig. 5E,F).

Interestingly, intact animals showed only minor impairment due to CSN silencing, which might be due to compensatory strategies that these animals were able to use when a subset of CSNs was inactivated (Fig. 5E,F).

Axotomized CSNs Increase Collateral Density in the Red Nucleus

To investigate whether the role of CSNs in reaching recovery is accompanied by novel relay projections made by these neurons after lesion and rehabilitative training, eYFP was specifically expressed in CSNs using the same Cre-dependent double AAV injections (Fig. 6A). Innervation density of the red nucleus was quantified on coronal sections through the midbrain for magno- and parvocellular parts as for the BDA traced cortical fibers (Fig. 6B). Regions of red nucleus innervation were selected on coronal projection plots (Fig. 6C,E) and fiber density analyzed. Animals that received a pyramidotomy and rehabilitative skilled reaching training showed a denser innervation of the parvocellular red nucleus than intact animals (Fig. 6D). A significant increase was found in lateral and ventral regions of the cup-shaped innervation area ($P < 0.05$). The magnocellular red nucleus was also significantly stronger innervated by CSN after pyramidotomy and rehabilitative training than in intact animals (Fig. 6F). In this part of the red nucleus, a stronger innervation increase was found medially ($P < 0.05$). In addition to increased innervation of the red nucleus, Rehab animals also showed stronger innervation of ventral parts of the nucleus raphe magnus and to a lesser extent the raphe pallidus above the lesion (Supplementary Fig. 3). These results suggest that axotomized CSNs increasingly relay their motor command via supra-lesional motor nuclei. To test for such a potential relay, the role of the cervically projecting RST in reaching recovery was investigated.

RSNs are Supporting Reaching Recovery after Pyramidotomy

To test whether red nucleus projections to the cervical spinal cord (RST) are an important substrate for reaching recovery in our paradigm, specific silencing of RSNs contralateral to the reaching paw was performed using hM4D. As for CSN silencing a Cre-dependent double AAV approach was used to ensure selective hM4D.mCherry expression in RSNs in intact animals (Intact) and animals that received a bilateral pyramidotomy and rehabilitative training (Rehab) (Fig. 7A). Reconstruction and counting of mCherry positive RSNs revealed a large amount of cells in the parvocellular and magnocellular parts of the red nucleus (~1000, Fig. 7B,C) in Rehab animals, while significantly less cells were detected in Intact animals (~320, $P < 0.01$) (Fig. 7C). Bilateral pyramidotomy led to a lesion deficit in pellet retrieval success score at 4/5 dpl ($P = 0.08$) which had recovered at 30 dpl with rehabilitative reaching training ($P < 0.05$) (Fig. 7D). When Rehab animals were tested after i.p. CNO injection, recovered reaching success dropped significantly by ~15% ($P < 0.05$, Fig. 7E). This effect was

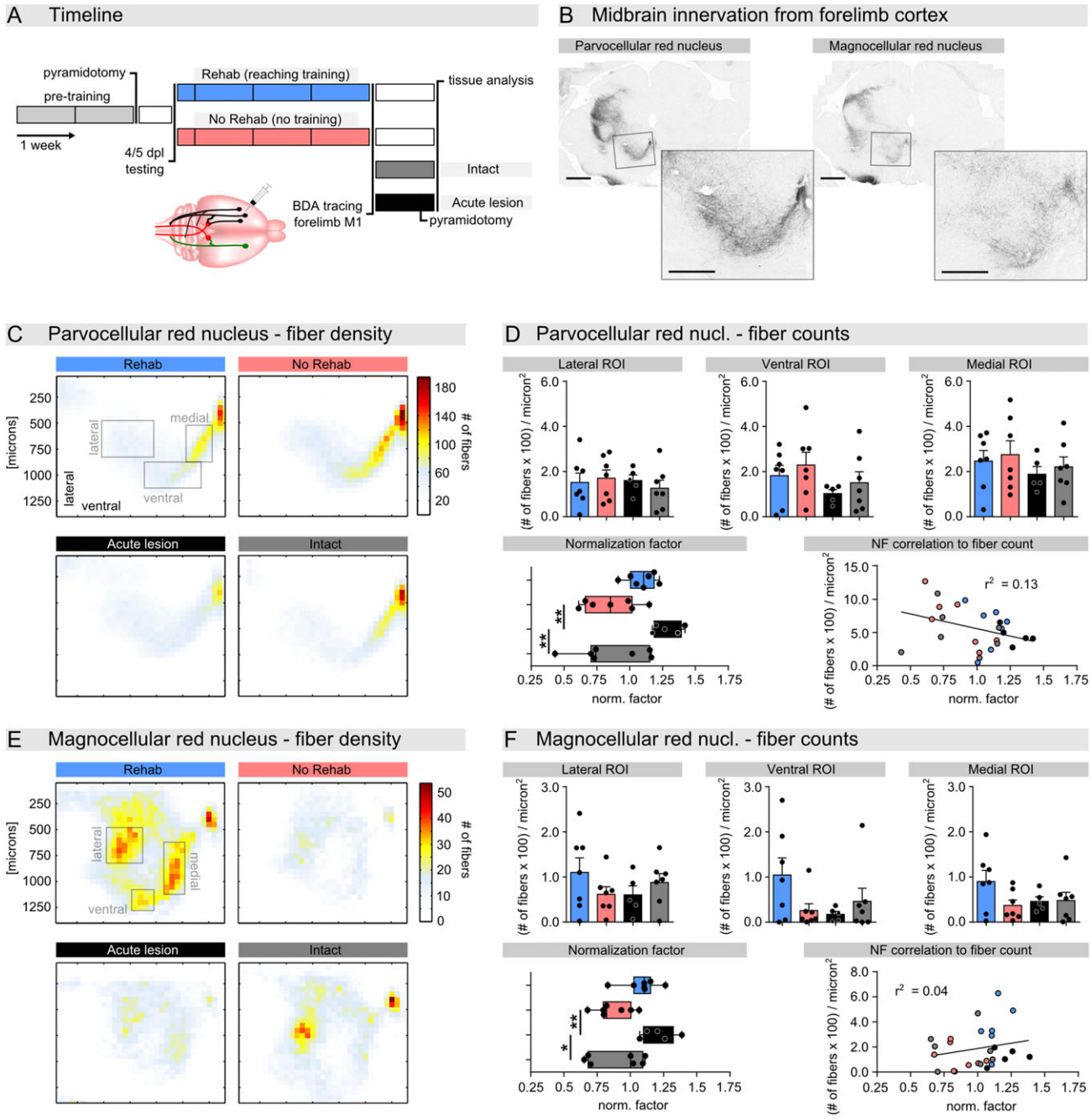

Figure 4. Total corticorubral innervation. (*A*) Experimental timeline. Skilled reaching trained animals received a bilateral pyramidotomy and rehabilitative reaching training (Rehab, blue, $n = 7$), or no training (No Rehab, red, $n = 7$) and were subsequently injected with BDA into the forelimb motor cortex 4 weeks post-lesion. An intact group (Intact, gray, $n = 7$) and an intact group receiving a bilateral pyramidotomy 5 days after BDA injection (Acute lesion, black, $n = 5$) were used as controls. All groups were perfused one week after BDA injection. (*B*) Coronal sections through the midbrain at the level of the parvocellular and magnocellular red nucleus (scale bar = 1000 μm). The boxed magnified areas show BDA positive fiber innervation of parvocellular and magnocellular parts of the red nucleus that were used for analysis (scale bar = 500 μm). (*C*) Group mean projection heat-plots indicating number of fibers per 250 μm^2 innervating the parvocellular red nucleus. Gray boxes indicate ROIs. (*D*) Fibers per μm^2 (×100) for each ROI in the parvocellular red nucleus normalized by the NF. No difference in innervation of the parvocellular red nucleus was found between groups for lateral (Rehab: 1.52 ± 0.41, No Rehab: 1.71 ± 0.36, Acute lesion: 1.60 ± 0.25, Intact: 1.26 ± 0.36), ventral (Rehab: 1.82 ± 0.45, No Rehab: 2.29 ± 0.56, Acute lesion: 1.03 ± 0.18, Intact: 1.51 ± 0.49), or medial ROI (Rehab: 2.46 ± 0.47, No Rehab: 2.75 ± 0.62, Acute lesion: 1.88 ± 0.34, Intact: 2.21 ± 0.44). The box plot shows the NF for each group. The NF of the Acute lesion group (1.29 ± 0.05) was significantly different from the NF of the No Rehab (0.86 ± 0.08, $P < 0.01$) and the Intact group (0.85 ± 0.10, $P < 0.01$). The summed fibers per μm^2 (×100) of all three ROIs are plotted against the NF to check effectiveness of normalization by correlating fiber density and staining intensity ($r^2 = 0.13$, ns). (*E*) Group mean projection heat-plots indicating number of fibers per 250 μm^2 bin innervating the magnocellular red nucleus. Gray boxes indicate ROIs. (*F*) Fibers per μm^2 (×100) for each ROI in the magnocellular red nucleus normalized by the NF. No significant difference was found between the groups despite the tendency in the Rehab group to show a stronger innervation in lateral (Rehab: 1.10 ± 0.32, No Rehab: 0.62 ± 0.17, Acute lesion: 0.60 ± 0.20, Intact: 0.88 ± 0.19), ventral (Rehab: 1.04 ± 0.38, No Rehab: 0.26 ± 0.15, Acute lesion: 0.17 ± 0.07, Intact: 0.46 ± 0.29), or medial ROI (Rehab: 0.90 ± 0.25, No Rehab: 0.37 ± 0.12, Acute lesion: 0.46 ± 0.10, Intact: 0.48 ± 0.18). The box plot shows the NF for each group. The NF of the Acute lesion group (1.08 ± 0.05) was significantly different from the NF of the No Rehab (0.87 ± 0.05, $P < 0.01$) and the Intact groups (0.90 ± 0.08, $P < 0.05$). The summed fibers per μm^2 (×100) of all three ROIs are plotted against the NF to check effectiveness of normalization by correlating fiber density and staining intensity ($r^2 = 0.04$, ns). One-way ANOVA, Bonferroni correction for multiple comparison. Two-tailed Pearson *r* was used to test for correlations. Box plot data are represented as median ± 25th percentile (box) and min/max (whiskers). Bar graph data are represented as means + SEM. Black or colored dots represent single animals.

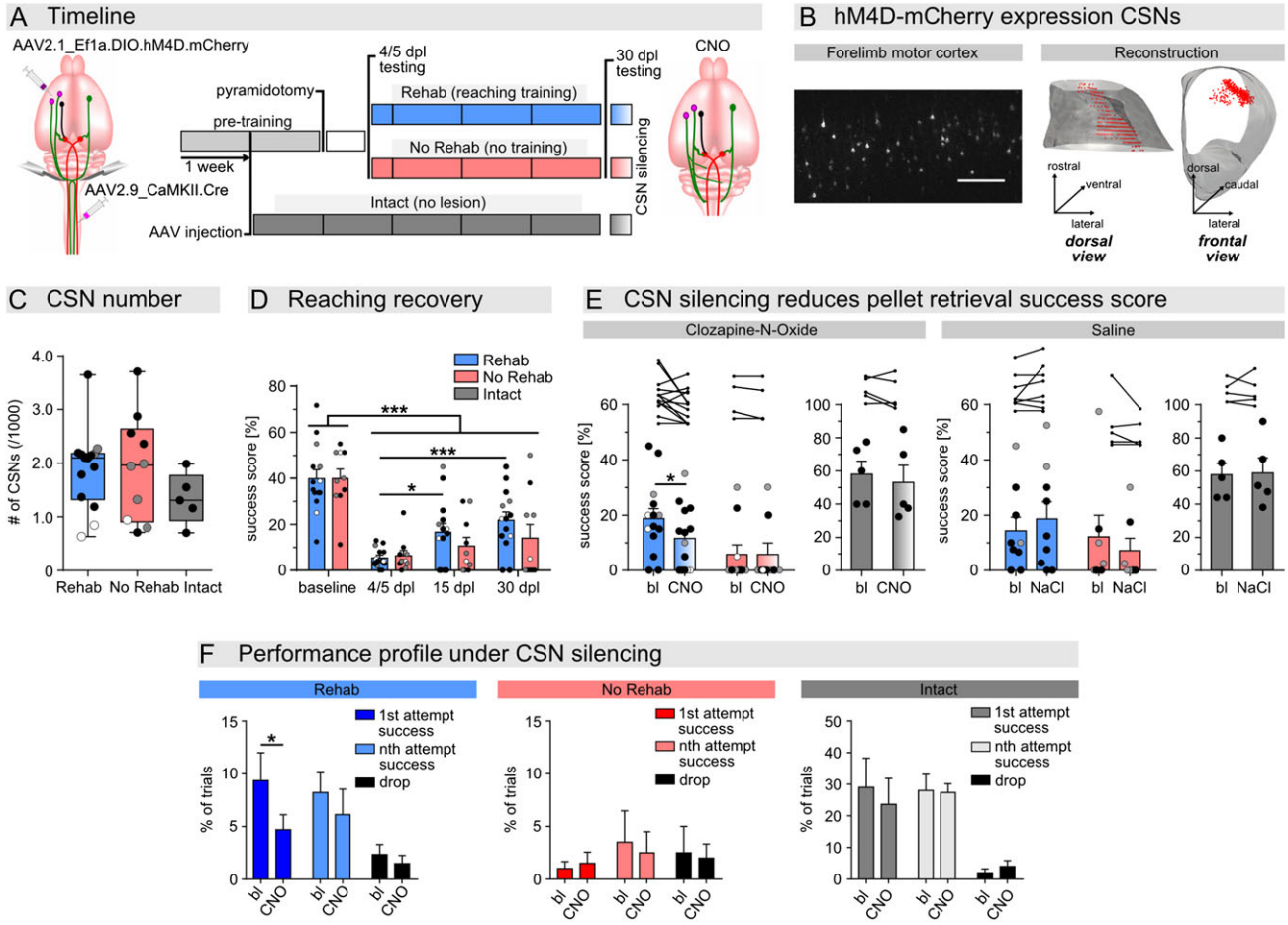

Figure 5. Effect of CSN silencing in chronic lesioned animals and intact animals. (*A*) Experimental design and timeline. Animals were injected with AAV2.9_CaMKII. Cre into the cervical spinal cord and Cre-dependent AAV2.1_Ef1a.DIO.hM4D.mCherry into the forelimb motor cortex ipsilateral and contralateral to the reaching paw, respectively. One week after AAV injections, skilled reaching trained animals received a bilateral pyramidotomy and rehabilitative training (Rehab, blue, $n = 14$) or no training (No Rehab, red, $n = 10$) until 4 weeks post-lesion. An intact control group (Intact, gray, $n = 5$) received only AAV injection but no lesion. Five weeks post AAV injection, all groups were tested in skilled reaching before and after CNO injection or saline injection. (*B*) CSNs in layer V of the forelimb motor cortex expressing mCherry (scale bar = 150 μm). Representative reconstruction of a hemisphere (gray) with mCherry expressing CSNs (red) in the forelimb motor cortex in a dorsal and frontal view. (*C*) Extrapolated numbers of mCherry expressing CSNs in forelimb motor cortex show no differences between groups (Rehab: 1897 ± 197, No Rehab: 1921 ± 312, Intact: 1342 ± 213; One-way ANOVA, $P = 0.37$). (*D*) Performance of skilled reaching after AAV injection and bilateral pyramidotomy. Rehab (baseline: 39.8% ± 4.0%, 4/5 dpl: 5.5% ± 1.1%) and No Rehab (baseline: 39.9% ± 4.2%, 4/5 dpl: 6.4% ± 2.3%) group showed a strong impairment in skilled reaching after pyramidotomy ($P < 0.001$). Only the Rehab group showed significant recovery over 4 weeks (15 dpl: 16.6% ± 3.8%, $P < 0.05$; 30 dpl: 21.9% ± 3.5%, $P < 0.001$), while the No Rehab group showed only slight improvements (15 dpl: 10.6% ± 3.8%; 30 dpl: 14.1% ± 5.9%). (*E*) CSN silencing under CNO and respective saline control. Rehab animals showed a significant reduction in the skilled reaching success score under CNO (bl: 18.8% ± 3.6%, CNO: 11.6% ± 3.0%, $n = 14$, $P < 0.05$) but not after saline injection (bl: 14.4% ± 5.0%, NaCl: 18.6% ± 6.2%, $n = 9$, $P = 0.44$). No Rehab and Intact animals did not show a significant reduction in skilled reaching performance under CNO (No Rehab: bl: 5.8% ± 3.5%, CNO: 5.0% ± 3.4%, $n = 10$, $P > 0.99$; Intact: bl: 58.0% ± 7.9%, CNO: 53.0% ± 10.4%, $n = 5$, $P = 0.49$) or saline (No Rehab: bl: 12.1% ± 7.9%, NaCl: 7.1% ± 4.5%, $n = 7$, $P = 0.42$; Intact: bl: 57.8% ± 6.8%, NaCl: 58.8% ± 9.1%, $n = 5$, $P = 0.88$). Inlets show single animals at baseline and under CNO/NaCl connected with lines. (*F*) Performance profiles under CSN silencing. CSN silencing led to a strongly reduced rate of first attempt successes in Rehab animals (bl: 9.4% ± 2.6%, CNO: 4.7% ± 1.4%, $P < 0.05$), while *n*th attempt successes and drops remained as frequent as during baseline testing. No Rehab and Intact animals showed no significant change in performance profiles under CNO testing. Two-way ANOVA rep. measures, Bonferroni correction for multiple comparison. Box plot data are represented as median ± 25th percentile (box) and min/max (whiskers). Bar graph data are represented as means + SEM. Dots represent single animals. White dots represent animals receiving AAV2.9_CaMKII.0.4.Cre.SV40 injection into the CST lesion site. Gray dots represent animals that were implanted with microwire electrode arrays.

not found when animals were injected with saline in the same manner. Unfortunately, the initial baseline performance on the day of saline testing was reduced compared with CNO baseline which might be due to daily performance changes and stresses the importance of comparison with same day baseline measurements. However, when single animals are compared before and during CNO/NaCl testing (Fig. 7*E* inlets) it becomes evident that only CNO reliably induced a drop in reaching success. Similar to the findings after CSN silencing, intact animals did not show a significant decrease in pellet retrieval success score with CNO. The lower number of cells infected by the AAV as well as compensatory strategies quickly adopted by intact animals might have contributed to this result. Interestingly, analysis of the performance profile during RSN silencing shows a strong decrease in *n*th attempt successes ($P < 0.001$), the non-missed outcome with the highest ratio at baseline, in both Rehab and Intact animals (Fig. 7*F*). First attempt successes as well as dropped trials remained unchanged under CNO. These results indicate that also RSN silencing mainly affected the successful targeting of the pellet in recovered and intact animals, leading to a strong decrease

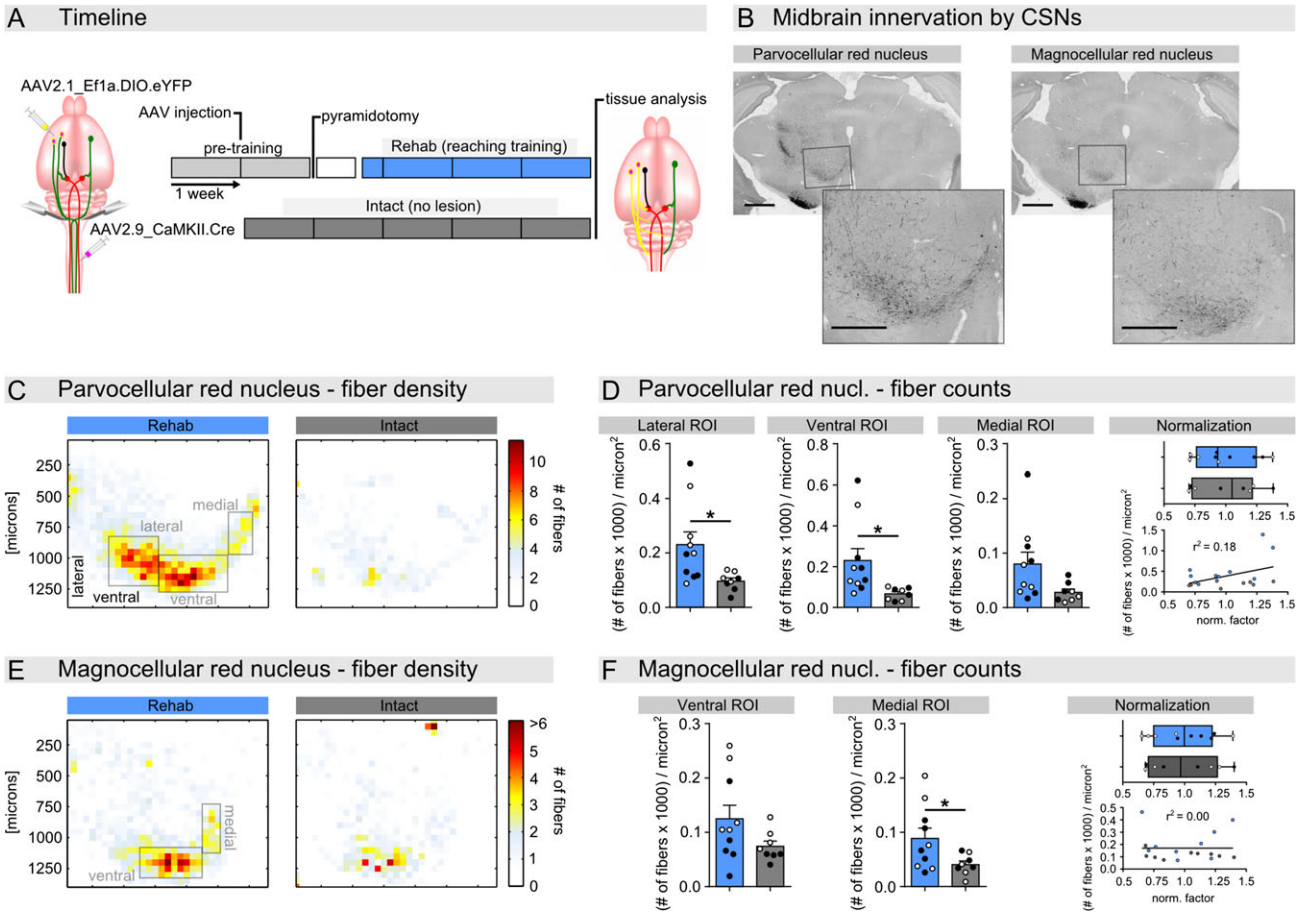

Figure 6. Specific corticorubral innervation by collaterals of CSNs. (*A*) Experimental design and timeline. Animals were injected with AAV2.9_CaMKII.Cre into the cervical spinal cord and Cre-dependent AAV2.1_Ef1a.DIO.eYFP into the forelimb motor cortex ipsilateral and contralateral to the reaching paw, respectively. One week after AAV injections, skilled reaching trained animals received a bilateral pyramidotomy and rehabilitative training (Rehab, blue, $n = 10$) until 4 weeks post-lesion. An intact control group (Intact, gray, $n = 8$) received only AAV injection but no lesion. Five weeks post AAV injection, both groups were perfused, and innervation of eYFP filled axons measured in the red nucleus. (*B*) Coronal sections through the midbrain at the level of the parvocellular and magnocellular red nucleus showing eYFP positive fiber innervation (scale bar = 1000 μm). The boxed magnified areas show eYFP positive fiber innervation of parvocellular and magnocellular parts of the red nucleus that were used for analysis (scale bar = 500 μm). (*C*) Group mean projection heat-plots indicating number of fibers per 250 μm^2 innervating the parvocellular red nucleus. Gray boxes indicate ROIs. (*D*) Fibers per μm^2 (×1000) for each ROI in the parvocellular red nucleus normalized by the NF. Lateral (Rehab: 2.31 ± 0.46, Intact: 0.96 ± 0.12) and ventral (Rehab: 2.30 ± 0.58, Intact: 0.67 ± 0.11) regions of the parvocellular red nucleus showed an increased innervation by CSNs in the Rehab group ($P < 0.05$), while the medial regions (Rehab: 0.80 ± 0.22, Intact: 0.28 ± 0.061) showed a strong tendency toward increased fiber density as well ($P = 0.055$). The box plot shows the NF for both groups with no difference between groups (Rehab: 0.99 ± 0.08, Intact: 1.00 ± 0.09). The summed fibers per μm^2 (×1000) of all three ROIs are plotted against the NF to check effectiveness of normalization by correlating fiber density and eYFP intensity ($r^2 = 0.18$, ns). (*E*) Group mean projection heat-plots indicating number of fibers per 250 μm^2 bin innervating the magnocellular red nucleus. Gray boxes indicate ROIs. (*F*) Fibers per μm^2 (×1000) for both ROIs in the magnocellular red nucleus normalized by the NF. Innervation of the medial region (Rehab: 0.89 ± 0.19, Intact: 0.41 ± 0.07) was significantly increased in the Rehab group compared with intact animals ($P < 0.05$), while the difference in the ventral region (Rehab: 1.25 ± 0.25, Intact: 0.74 ± 0.10) was less profound ($P = 0.11$). The box plot shows the NF for both groups with no difference between groups (Rehab: 1.00 ± 0.08, Intact: 1.00 ± 0.10). The summed fibers per μm^2 (×1000) of both ROIs are plotted against the NF to check effectiveness of normalization by correlating fiber density and eYFP intensity ($r^2 = 0.00$, ns). One-way ANOVA, Bonferroni correction for multiple comparison. Two-tailed Pearson *r* was used to test for correlations. Box plot data are represented as median ± 25th percentile (box) and min/max (whiskers). Bar graph data are represented as means + SEM. Dots represent single animals. White dots represent animals additionally injected with AAV2.1_Ef1a.DIO.hM4D.mCherry.

in the overall success rate in the Rehab group. This significant drop in performance after RSN silencing, suggests a crucial role of the RST in skilled reaching after bilateral pyramidotomy and rehabilitative training.

Discussion

Rehabilitative Training Leads to Functional Recovery of Skilled Reaching after Pyramidotomy

In the present study, we report evidence for a crucial role of a cortical relay for the recovery of skilled reaching after bilateral pyramidotomy. Performing daily rehabilitative training of skilled reaching over 4 weeks led to significantly higher levels of recovery than in the non-trained controls. Such strong recovery has rarely been described after bilateral pyramidotomy in rats (Weidner et al. 2001), except with plasticity-inducing therapies, such as chondroitinase or anti-Nogo-A antibodies (Thallmair et al. 1998; Raineteau et al. 2001; Garcia-Alias et al. 2009). In contrast to these earlier experiments, our reaching setup did not allow animals to compensate for lost function by scooping pellets from the pedestal or dropping them and eating from the floor. Analysis of the reaching skill levels on non-missed trials revealed that Rehab animals were better capable

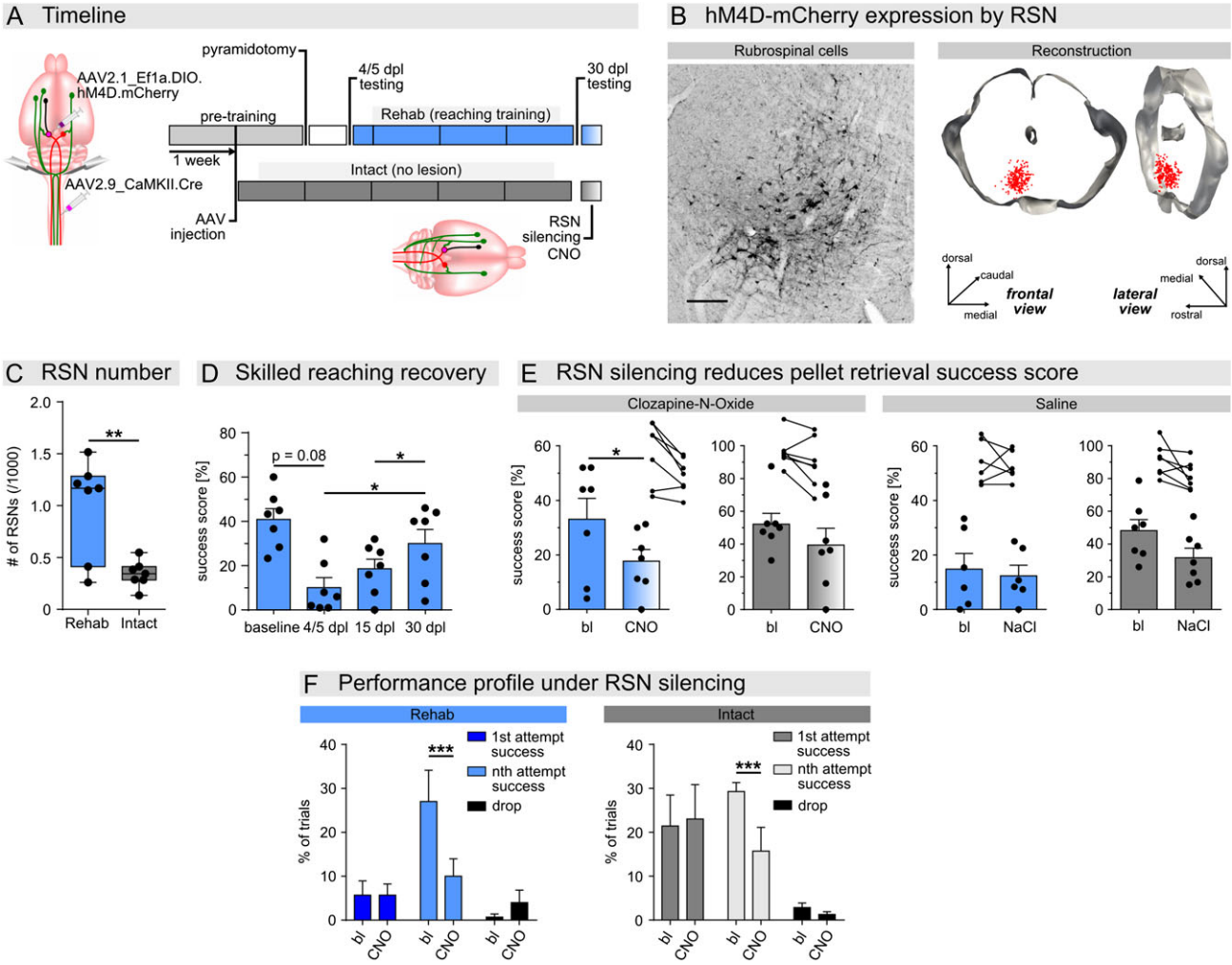

Figure 7. Effect of RSN silencing on reaching success in lesioned and intact animals. (*A*) Experimental design and timeline. Animals were injected with AAV2.9_CaMKII. Cre into the cervical spinal cord and Cre-dependent AAV2.1_Ef1a.DIO.hM4D.mCherry into the red nucleus ipsilateral and contralateral to the reaching paw, respectively. One week after AAV injections, skilled reaching trained animals received a bilateral pyramidotomy and rehabilitative training (Rehab, blue, $n = 7$) until 4 weeks post-lesion, or no lesion (Intact, gray, $n = 7$). Animals were then tested in skilled reaching before and after CNO injection or saline injection. (*B*) RSNs expressing mCherry detected by immunohistochemistry (scale bar = 100 μm). Representative reconstruction of the midbrain (gray) with mCherry expressing RSNs (red) in a frontal and side view. (*C*) Extrapolated numbers of mCherry expressing RSNs show a mean value of 1000 ± 178 cells in Rehab animals and a significantly smaller number of cells (342 ± 128, $P < 0.01$) in Intact animals. (*D*) Performance of skilled reaching after AAV injection and bilateral pyramidotomy. Animals showed a profound impairment in skilled reaching after pyramidotomy (baseline: 41.0% ± 4.8%, 4/5 dpl: 10.1% ± 4.5%, $P = 0.08$) and significant recovery over 4 weeks of rehabilitative training (15 dpl: 18.6% ± 4.3%; 30 dpl: 30.0% ± 6.3%, $P < 0.05$). (*E*) RSN silencing under CNO and respective saline controls. Rehab animals showed a significant impairment in single pellet retrieval success score under CNO (bl: 33.1% ± 7.7%, CNO: 17.7% ± 4.3%, $P < 0.05$, $n = 7$) but not after saline injection (bl: 14.8% ± 5.8%, NaCl: 12.3% ± 3.9%, $P = 0.70$, $n = 6$). Intact animals did not show a significant drop in success rate under CNO (bl: 52.1% ± 6.6%, CNO: 39.4% ± 10.3%, $P = 0.1$) or saline (bl: 48.1% ± 6.8%, NaCl: 31.7% ± 5.8%, $P = 0.08$). Inlets show single animals at baseline and under CNO/NaCl connected with lines. (*F*) Performance profile at baseline and during RSN silencing shows a strong decrease in the rate of *n*th attempt successes in Rehab (bl: 27.0% ± 7.2%, CNO: 10.0% ± 4.0%, $P < 0.001$) and Intact animals (bl: 29.3% ± 2.0%, CNO: 15.7% ± 5.4%, $P < 0.001$). One-way and two-way ANOVA rep. measures, Bonferroni correction for multiple comparison. Paired and unpaired Student's *t*-test. Box plot data are represented as median ± 25th percentile (box) and min/max (whiskers). Bar graph data are represented as means + SEM. Black dots represent single animals.

of targeting the pellet and bringing it securely to their mouth, while more No Rehab animals frequently dropped the grasped pellet. Thus, the here-described training-induced recovery represents a regain of forelimb motor skill which exceeds spontaneous recovery in success score and quality. We have used several functional readouts to elucidate the role of remaining cortical activity in mediating this observed reaching recovery.

Forelimb Motor Cortex Maintains a Crucial Role in Skilled Reaching

When motor cortex was destroyed by a stroke lesion after animals had recovered from a bilateral pyramidotomy, skilled reaching performance dropped by more than 50% of its original value. This finding differs from that of an earlier study (Fanardjian et al. 2000), where animals that had received pretraining in balancing on a rotating bar recovered within 1 day from a unilateral pyramidotomy and a consecutive motor cortex stroke, but took much longer to recover from a stroke alone. The authors hypothesized that the recovery from the unilateral pyramidotomy occurred by the RST fully taking over the motor control, thus leaving the following stroke lesion without much consequence. Further, a more recent study using forelimb timed lever pressing with no need for dexterity found that a motor cortex stroke did not affect performance once the skill was learned, but prevented learning if induced before training (Kawai et al. 2015). Both studies suggest that

subcortical motor structures can take over the full control of certain skilled movements, rendering the behavior cortically independent. Yet, when animals were pretrained in skilled reaching, recovery from a forelimb motor cortex stroke was slower than when animals were newly learning the task after stroke, without having had pretraining (Schubring-Giese et al. 2007). This finding suggests that during retraining of skilled reaching the cortical motor command had to be laboriously shifted from the damaged cortical areas to intact ones. In contrast, when the motor skill was learned only after stroke, it was encoded in intact cortical areas from the beginning, leading to a faster learning process. Furthermore, a recent study has reported that after a cervical dorsal quadrant lesion (including the CST) animals that were pretrained in skilled reaching showed increased training-induced recovery compared with animals naïve to the task before the lesion (May et al. 2015), suggesting that when the cortex is not directly affect by the injury, rerouting of stable cortical control via intact descending tracts is faster than newly learning the skill after injury. Our findings after pyramidotomy support this view of cortex-dependent control of reaching during rehabilitative training.

By recording activity in layer V in the forelimb motor cortex during skilled reaching, we found that the same cortical regions as before the lesion were activated during recovery. Lesioning of the CST induced only a transient reduction in digit flexion-related cortical activity, which reappeared gradually in the original cortical subregions. In parallel to the re-establishment of this reach-related activity an increase in reaching success rate occurred, suggesting that when the cortical activity recovered, motor control improved. These findings suggest that no major reorganization took place in forelimb motor cortex after CST axotomy in the brainstem. This is in contrast to results from thoracic spinal cord injury studies, where substantial topographic reorganization of the hindlimb motor cortex and formation of new forelimb and hindlimb motor maps has been found (Fouad et al. 2001; Bareyre et al. 2004; Ghosh et al. 2010). However, it is important to note that this reorganization occurred in a context during which the animal was forced to increase its forelimb strength due to impairment of its hindlimbs. Recent studies showed that when the hindlimb motor cortex is actively trained in a virtual hindlimb lever press task, pre-lesion activity reoccurs even after complete spinal cord injury (Manohar et al. 2012; Knudsen et al. 2014). Here, we found that during rehabilitative training reach-related activity in motor cortex stabilized shortly after a pyramidotomy, suggesting that original cortical motor control of skilled reaching behavior is re-recruited after pyramidotomy. Interestingly, two recent studies found re-establishment of cortical stimulation evoked motor responses after lesions in the internal capsule (Ishida et al. 2016) and the cervical dorsal columns (Hilton et al. 2016) after a similar (1–2 week) post-lesion period. As our recordings were targeted to the caudal forelimb area of motor cortex, from which the main direct cortical control over cervical spinal cord arises, an increased cortical reorganization in the rostral forelimb area could have accompanied the recovery. This possibility remains to be investigated in future studies.

Yet, the cortical motor commands measured in our animals must all have been relayed via subcortical spinally projecting motor nuclei to allow functional control, due to the complete CST axotomy performed here. We therefore investigated potential increase in innervation of such motor nuclei.

Bulk Corticorubral Innervation is Only Slightly Affected by Pyramidotomy and Training

By anterograde tracing of forelimb motor cortex projections, only a trend but no significant increase in fiber density in the red nucleus was found after injury and rehabilitative training. Earlier studies have described increased corticorubral innervation from the axotomized cortex after unilateral pyramidotomy and anti-Nogo-A antibody treatment, but mainly found axon growth toward the contralateral red nucleus (Thallmair et al. 1998; Z'Graggen et al. 1998). Considering the crossed projection of the RST, innervation of the ipsilateral red nucleus could provide a more direct relay from motor cortex. In a recent study on unilateral lesions of the internal capsule, a causal role of such ipsilateral (and ipsilesional) corticorubral sprouting in forelimb recovery was established using a genetic neuronal silencing approach (Ishida et al. 2016). When the intact hemisphere was electrically stimulated after a unilateral pyramidotomy, corticorubral sprouting was found in the ipsilateral and contralateral red nucleus (Carmel et al. 2013) with highest fiber densities in medial areas. With rehabilitative training we here describe a similar tendency in the ipsilateral magnocellular red nucleus. Ventral and medial parts of the red nucleus were more strongly innervated in some animals of the Rehab group than in other groups, but the overall group difference was not significant. Instead, we found significant sprouting and evidence for a crucial role in recovery of reaching the axotomized CSNs, representing only a small fraction of corticorubral projecting cells.

Axotomized CSNs Support Recovery of Skilled Reaching

A potential role of CSNs in recovery after pyramidotomy requires the long-term survival of CSNs after axotomy. CSN survival has been extensively studied after thoracic injuries in the past (Barron et al. 1988; Hains et al. 2003; Nielson et al. 2010, 2011; Oudega and Perez 2012). In mice, CSNs were found to survive long-term after axotomy in the brainstem, but showed synaptic loss (Ghosh et al. 2012). However, internal capsule lesions led to persistent cell death in adult rats (Bonatz et al. 2000). These findings suggest that cell death depends on the proximity of axotomy to the cell body and trophic support from other target areas. Here, we found no difference in the number of CSNs retrogradely traced from the lesion site after pyramidotomy 1 and 5 weeks after the injury. Additionally, numbers of CSNs expressing mCherry were similar in intact and lesioned animals. These two results provide evidence that CSNs survive after axotomy in the brainstem and support our finding of their functional role in behavior.

We have specifically targeted forelimb CSNs to express an inhibitory chemogenetic hM4D silencing construct. Acute silencing of CSNs after recovery from axotomy led to a significant decrease in skilled reaching performance in Rehab animals. While similar in absolute numbers, the deficit was smaller than the one induced by lesioning the full motor cortex when compared relative to their respective baseline. However, using the retrograde infection technique, only CSNs projecting to C4–C6 in the spinal cord were reached and expressed the inhibitory hM4D. Spinal segments C4–C6 contain motorneuron pools innervating both proximal and distal forelimb muscles, but forelimb motorneuron pools extend from C2-T1 (McKenna et al. 2000). The silencing deficit could thus be bigger if all cervically projecting neurons could be silenced. The result that the deficit was significant when silencing a subpopulation of forelimb CSNs suggests a strong role of these cells in reaching recovery.

Over all experiments and groups, the double AAV injection approach had a noticeable effect on the reaching success shortly after injection at baseline and also after bilateral pyramidotomy. We found a slight reduction in recovery levels in Rehab animals, and a reduced recovery in No Rehab animals. The minimal recovery in No Rehab animals did not allow the detection of a further deficit with silencing of CSNs; therefore, the role of CSNs in spontaneous recovery remains uncertain.

Interestingly, in intact animals, silencing of this C4–C6 subpopulation of CSNs only led to an insignificant small reduction in pellet retrieval success score, providing further evidence that recovery of skilled reaching depends substantially on CSNs, while intact animals are able to compensate for silencing of these neurons.

Axotomized CSNs Increase Supra-Lesional Innervation

Using Cre-dependent eYFP expression to selectively label the processes of the axotomized CSNs, we found a strong increase of collateral innervation density of the red nucleus by the axotomized CSNs in Rehab animals compared with intact animals. In intact animals, only very few CST collaterals were found. This finding is in accordance with a previous retrograde tracing study in rats (Akintunde and Buxton 1992). It is beyond the scope of techniques used here to elucidate whether this increased density is due to newly formed fibers growing from the main CST axon, or due to arborization of the few already existing collaterals.

Rehabilitative skilled reaching training after pyramidotomy was accompanied by sprouting of CSNs in the parvocellular and magnocellular parts of the red nucleus. Parvocellular areas were most strongly innervated ventrally and ventrolaterally, while magnocellular innervation was most enhanced in medial regions. Accordingly, retrograde tracing in mice has shown that neurons projecting to the spinal cord are mainly located in ventrolateral rostral and dorsomedial caudal parts of the red nucleus (Liang et al. 2012). Furthermore, rubrospinal fibers from medial parts of the red nucleus have been shown to project mainly to cervical spinal segments, while ventral and lateral parts project to the lumbar cord (Brown 1974b; Liang et al. 2012). Innervation from forelimb CSNs was increased in both these locations. Furthermore, in our animals, mCherry expressing retrogradely labeled RSNs, projecting to cervical segments, were mainly located in ventromedial areas along the rostrocaudal axis of the red nucleus, overlapping with the increased CSN innervation density. Taken together, these findings suggest the formation of a strong corticorubrospinal relay by axotomized corticospinal fibers. It is to be mentioned however, that increased CST collateral innervation of red nucleus neurons that project to the inferior olive and participate in the cerebellar loop did likely also occur and is indistinguishable with the approaches used here.

In addition to increased rubral innervation, an increase in fiber density in the raphe nuclei was found. A recent study using mouse mutants with enhanced plasticity described increased sprouting of rubral fibers into raphe nuclei, along with increased innervation of the pons and cervical spinal cord after bilateral pyramidotomy (Siegel et al. 2015). Silencing of the raphe magnus led to an increased impairment in skilled walking in these animals. Furthermore, the medullary reticular formation has recently been shown to be important for skilled reaching (Esposito et al. 2014). However, the MdV is located below the level of lesion in our model and could thus not serve as relay for CSNs here. For skilled reaching recovery, the red nucleus provides an anatomically and functionally optimal relay station for cortical motor control, and is known to be able to increase sprouting into the cervical cord after pyramidotomy (Raineteau et al. 2002; Siegel et al. 2015).

RSNs are Crucial for Recovered Skilled Reaching after Bilateral Pyramidotomy

Transient silencing of RSNs projecting to the cervical spinal cord led to a strong deficit in recovered skilled reaching performance, which exceeded the deficit induced by RSN silencing in intact animals. Importantly, our viral approach of targeting RSNs led to significantly less mCherry positive cells in Intact than in Rehab animals. This could be due to technical reasons, but might also imply a possible RST sprouting response in Rehab animals that led to more virus uptake in the spinal cord. Cell counts after retrograde tracing from spinal cord have been previously used by our group to determine spinal sprouting response after injury (Bachmann et al. 2014; Lindau et al. 2014; Zorner et al. 2014). However, in the experiments performed here, the spinal virus injection was performed up to a week before the pyramidotomy and it is unlikely that sprouting occurring some weeks later would lead to increased uptake of virus residual in the tissue.

Interestingly, and supported by our findings in intact animals here, lesions to the RST have been described to induce only mild impairments in skilled reaching in intact animals (Whishaw et al. 1992b; Morris et al. 2011, 2015; Morris and Whishaw 2016), and to add only minor deficits when performed simultaneously to a motor cortex stroke lesion (Whishaw et al. 1990). Furthermore, a recent retrograde tracing study in mice counted ~2100 cells in the red nucleus that project to the cervical spinal cord (Liang et al. 2012). If these numbers can be adapted from the mouse, our silencing approach affected less than half of the cervically projecting RSNs in Rehab animals. The observed impairment of recovered reaching skill by silencing a subpopulation of RSNs therefore provides evidence for a crucial role of this tract in mediating recovery.

Importantly, recovery achieved by rehabilitative training in our animals was not 100%. The reorganization after bilateral pyramidotomy does not allow the same fine motor skill as the intact CST. Whether other therapies together with rehabilitative training might induce a higher level of plasticity and functional recovery remains to be studied (Wahl et al. 2014). Furthermore, neither silencing the motor cortex, CSNs, or RSNs alone induced a full incapability of skilled reaching. Other subcortical motor systems (Alstermark and Pettersson 2014; Azim et al. 2014; Esposito et al. 2014) or motor cortex contralateral to the reaching paw thus presumably still provided some forelimb control, which will have to be addressed in future studies.

In summary, we show increased functional recovery of skilled forelimb reaching in animals with a complete bilateral brainstem CST lesion, achieved by intense rehabilitative training. We found that motor cortex control over skilled reaching remains strong after this lesion, and cortical reach-related activity stably reappears with recovery. The recovered reaching performance strongly depends on the axotomized CSNs which we show to increase their density of collaterals in the red nucleus and brainstem. Despite being low in number compared with the bulk of corticobulbar connections, supra-lesional collaterals of CSNs as well as cervically projecting RSNs were found to play a key role in the recovered reaching skill (Supplementary Fig. 4).

Conceptually, our findings suggest that training-induced recovery makes use of established motor circuits, a mode of

recovery termed "resuscitation" (Kleim 2011). In patients with spinal cord injury, such activation can also be achieved by rehabilitative training and during motor imagery (Alkadhi et al. 2005). A recent patient case study found that motor imagery training can lead to increased performance in a reaching task after spinal cord injury (Grangeon et al. 2012). Thus reactivation of a stably encoded motor engram, silenced by the injury, can have profound effects on recovery of skilled movements.

Supplementary Material

Supplementary material is available at *Cerebral Cortex* online.

Funding

The Swiss National Science Foundation Grant (31003A_149315); the European Research Council Grant (294115 NOGORISE); the ETH Research Grant (0-20932-13); and the Christopher and Dana Reeve Foundation.

Notes

The authors thank Dr Arko Ghosh for valuable discussions and providing the Multichannel Systems electrophysiology setup; Dr Wolfger Von der Behrens for support with analysis of electrophysiological data; Anna Jeske, Hansjörg Kasper, Martin Wieckhorst, and Marco Tedaldi for technical support; and Dr Shane A. Liddelow for proof reading of the manuscript. *Conflict of Interest*: None declared.

References

Akintunde A, Buxton DF. 1992. Origins and collateralization of corticospinal, corticopontine, corticorubral and corticostriatal tracts: a multiple retrograde fluorescent tracing study. Brain Res. 586:208–218.

Alkadhi H, Brugger P, Boendermaker SH, Crelier G, Curt A, Hepp-Reymond MC, Kollias SS. 2005. What disconnection tells about motor imagery: evidence from paraplegic patients. Cereb Cortex. 15:131–140.

Alstermark B, Pettersson LG. 2014. Skilled reaching and grasping in the rat: lacking effect of corticospinal lesion. Front Neurol. 5:103.

Anderson KD, Gunawan A, Steward O. 2005. Quantitative assessment of forelimb motor function after cervical spinal cord injury in rats: relationship to the corticospinal tract. Exp Neurol. 194:161–174.

Azim E, Jiang J, Alstermark B, Jessell TM. 2014. Skilled reaching relies on a V2a propriospinal internal copy circuit. Nature. 508:357–363.

Bachmann LC, Lindau NT, Felder P, Schwab ME. 2014. Sprouting of brainstem-spinal tracts in response to unilateral motor cortex stroke in mice. J Neurosci. 34:3378–3389.

Bareyre FM, Kerschensteiner M, Raineteau O, Mettenleiter TC, Weinmann O, Schwab ME. 2004. The injured spinal cord spontaneously forms a new intraspinal circuit in adult rats. Nat Neurosci. 7:269–277.

Barron KD, Dentinger MP, Popp AJ, Mankes R. 1988. Neurons of layer Vb of rat sensorimotor cortex atrophy but do not die after thoracic cord transection. J Neuropathol Exp Neurol. 47:62–74.

Bonatz H, Rohrig S, Mestres P, Meyer M, Giehl KM. 2000. An axotomy model for the induction of death of rat and mouse corticospinal neurons in vivo. J Neurosci Methods. 100: 105–115.

Brown LT. 1974a. Corticorubral projections in the rat. J Comp Neurol. 154:149–167.

Brown LT. 1974b. Rubrospinal projections in the rat. J Comp Neurol. 154:169–187.

Brus-Ramer M, Carmel JB, Chakrabarty S, Martin JH. 2007. Electrical stimulation of spared corticospinal axons augments connections with ipsilateral spinal motor circuits after injury. J Neurosci. 27:13793–13801.

Buitrago MM, Ringer T, Schulz JB, Dichgans J, Luft AR. 2004. Characterization of motor skill and instrumental learning time scales in a skilled reaching task in rat. Behav Brain Res. 155:249–256.

Cafferty WB, Strittmatter SM. 2006. The Nogo-Nogo receptor pathway limits a spectrum of adult CNS axonal growth. J Neurosci. 26:12242–12250.

Carmel JB, Berrol LJ, Brus-Ramer M, Martin JH. 2010. Chronic electrical stimulation of the intact corticospinal system after unilateral injury restores skilled locomotor control and promotes spinal axon outgrowth. J Neurosci. 30:10918–10926.

Carmel JB, Kimura H, Berrol LJ, Martin JH. 2013. Motor cortex electrical stimulation promotes axon outgrowth to brain stem and spinal targets that control the forelimb impaired by unilateral corticospinal injury. Eur J Neurosci. 37: 1090–1102.

Dolbakyan E, Hernandez-Mesa N, Bures J. 1977. Skilled forelimb movements and unit activity in motor cortex and caudate nucleus in rats. Neuroscience. 2:73–80.

Esposito MS, Capelli P, Arber S. 2014. Brainstem nucleus MdV mediates skilled forelimb motor tasks. Nature. 508:351–356.

Fanardjian VV, Gevorkyan OV, Mallina RK, Melik-Moussian AB, Meliksetyan IB. 2000. Enhanced behavioral recovery from sensorimotor cortex lesions after pyramidotomy in adult rats. Neural Plast. 7:261–277.

Fouad K, Pedersen V, Schwab ME, Brosamle C. 2001. Cervical sprouting of corticospinal fibers after thoracic spinal cord injury accompanies shifts in evoked motor responses. Curr Biol. 11:1766–1770.

Freund P, Schneider T, Nagy Z, Hutton C, Weiskopf N, Friston K, Wheeler-Kingshott CA, Thompson AJ. 2012. Degeneration of the injured cervical cord is associated with remote changes in corticospinal tract integrity and upper limb impairment. PLoS One. 7:e51729.

Friedli L, Rosenzweig ES, Barraud Q, Schubert M, Dominici N, Awai L, Nielson JL, Musienko P, Nout-Lomas Y, Zhong H, et al. 2015. Pronounced species divergence in corticospinal tract reorganization and functional recovery after lateralized spinal cord injury favors primates. Sci Transl Med. 7: 302ra134.

Garcia-Alias G, Barkhuysen S, Buckle M, Fawcett JW. 2009. Chondroitinase ABC treatment opens a window of opportunity for task-specific rehabilitation. Nat Neurosci. 12: 1145–1151.

Ghosh A, Haiss F, Sydekum E, Schneider R, Gullo M, Wyss MT, Mueggler T, Baltes C, Rudin M, Weber B, et al. 2010. Rewiring of hindlimb corticospinal neurons after spinal cord injury. Nat Neurosci. 13:97–104.

Ghosh A, Peduzzi S, Snyder M, Schneider R, Starkey M, Schwab ME. 2012. Heterogeneous spine loss in layer 5 cortical neurons after spinal cord injury. Cereb Cortex. 22: 1309–1317.

Grangeon M, Revol P, Guillot A, Rode G, Collet C. 2012. Could motor imagery be effective in upper limb rehabilitation of individuals with spinal cord injury? A case study. Spinal Cord. 50:766–771.

Gwyn DG, Flumerfelt BA. 1974. A comparison of the distribution of cortical and cerebellar afferents in the red nucleus of the rat. Brain Res. 69:130–135.

Hains BC, Black JA, Waxman SG. 2003. Primary cortical motor neurons undergo apoptosis after axotomizing spinal cord injury. J Comp Neurol. 462:328–341.

Han Q, Cao C, Ding Y, So KF, Wu W, Qu Y, Zhou L. 2015. Plasticity of motor network and function in the absence of corticospinal projection. Exp Neurol. 267:194–208.

Hepp R, Trouche E, Wiesendanger M. 1974. Effects of unilateral and bilateral pyramidotomy on a conditioned rapid precision grip in monkeys (Macaca fascicularis). Exp Brain Res. 21:519–527.

Hilton BJ, Anenberg E, Harrison TC, Boyd JD, Murphy TH, Tetzlaff W. 2016. Re-establishment of cortical motor output maps and spontaneous functional recovery via spared dorsolaterally projecting corticospinal neurons after dorsal column spinal cord injury in adult mice. J Neurosci. 36: 4080–4092.

Hyland B. 1998. Neural activity related to reaching and grasping in rostral and caudal regions of rat motor cortex. Behav Brain Res. 94:255–269.

Isa T, Kinoshita M, Nishimura Y. 2013. Role of direct vs. indirect pathways from the motor cortex to spinal motoneurons in the control of hand dexterity. Front Neurol. 4:191.

Ishida A, Isa K, Umeda T, Kobayashi K, Kobayashi K, Hida H, Isa T. 2016. Causal link between the cortico-rubral pathway and functional recovery through forced impaired limb use in rats with stroke. J Neurosci. 36:455–467.

Kanagal SG, Muir GD. 2009. Task-dependent compensation after pyramidal tract and dorsolateral spinal lesions in rats. Exp Neurol. 216:193–206.

Kawai R, Markman T, Poddar R, Ko R, Fantana AL, Dhawale AK, Kampff AR, Olveczky BP. 2015. Motor cortex is required for learning but not for executing a motor skill. Neuron. 86: 800–812.

Kennedy PR. 1990. Corticospinal, rubrospinal and rubro-olivary projections: a unifying hypothesis. Trends Neurosci. 13: 474–479.

Kleim JA. 2011. Neural plasticity and neurorehabilitation: teaching the new brain old tricks. J Commun Disord. 44:521–528.

Klein A, Sacrey LA, Whishaw IQ, Dunnett SB. 2012. The use of rodent skilled reaching as a translational model for investigating brain damage and disease. Neurosci Biobehav Rev. 36:1030–1042.

Knudsen EB, Powers ME, Moxon KA. 2014. Dissociating movement from movement timing in the rat primary motor cortex. J Neurosci. 34:15576–15586.

Kralik JD, Dimitrov DF, Krupa DJ, Katz DB, Cohen D, Nicolelis MAL. 2001. Techniques for long-term multisite neuronal ensemble recordings in behaving animals. Methods. 25:121–150.

Lang CE, Schieber MH. 2003. Differential impairment of individuated finger movements in humans after damage to the motor cortex or the corticospinal tract. J Neurophysiol. 90:1160–1170.

Lawrence DG, Kuypers HG. 1968a. The functional organization of the motor system in the monkey. I. The effects of bilateral pyramidal lesions. Brain. 91:1–14.

Lawrence DG, Kuypers HG. 1968b. The functional organization of the motor system in the monkey. II. The effects of lesions of the descending brain-stem pathways. Brain. 91:15–36.

Liang H, Paxinos G, Watson C. 2012. The red nucleus and the rubrospinal projection in the mouse. Brain Struct Funct. 217: 221–232.

Lindau NT, Banninger BJ, Gullo M, Good NA, Bachmann LC, Starkey ML, Schwab ME. 2014. Rewiring of the corticospinal tract in the adult rat after unilateral stroke and anti-Nogo-A therapy. Brain. 137:739–756.

Liu K, Lu Y, Lee JK, Samara R, Willenberg R, Sears-Kraxberger I, Tedeschi A, Park KK, Jin D, Cai B, et al. 2010. PTEN deletion enhances the regenerative ability of adult corticospinal neurons. Nat Neurosci. 13:1075–1081.

Ludwig KA, Miriani RM, Langhals NB, Joseph MD, Anderson DJ, Kipke DR. 2009. Using a common average reference to improve cortical neuron recordings from microelectrode arrays. J Neurophysiol. 101:1679–1689.

Ma VY, Chan L, Carruthers KJ. 2014. Incidence, prevalence, costs, and impact on disability of common conditions requiring rehabilitation in the United States: stroke, spinal cord injury, traumatic brain injury, multiple sclerosis, osteoarthritis, rheumatoid arthritis, limb loss, and back pain. Arch Phys Med Rehabil. 95:986–995 e981.

Maier IC, Baumann K, Thallmair M, Weinmann O, Scholl J, Schwab ME. 2008. Constraint-induced movement therapy in the adult rat after unilateral corticospinal tract injury. J Neurosci. 28:9386–9403.

Manohar A, Flint RD, Knudsen E, Moxon KA. 2012. Decoding hindlimb movement for a brain machine interface after a complete spinal transection. PLoS One. 7:e52173.

Maraka S, Jiang Q, Jafari-Khouzani K, Li L, Malik S, Hamidian H, Zhang T, Lu M, Soltanian-Zadeh H, Chopp M, et al. 2014. Degree of corticospinal tract damage correlates with motor function after stroke. Ann Clin Transl Neurol. 1:891–899.

May Z, Fouad K, Shum-Siu A, Magnuson DS. 2015. Challenges of animal models in SCI research: Effects of pre-injury task-specific training in adult rats before lesion. Behav Brain Res. 291:26–35.

McKenna JE, Prusky GT, Whishaw IQ. 2000. Cervical motoneuron topography reflects the proximodistal organization of muscles and movements of the rat forelimb: a retrograde carbocyanine dye analysis. J Comp Neurol. 419:286–296.

Mori M, Kose A, Tsujino T, Tanaka C. 1990. Immunocytochemical localization of protein kinase C subspecies in the rat spinal cord: light and electron microscopic study. J Comp Neurol. 299:167–177.

Morris R, Tosolini AP, Goldstein JD, Whishaw IQ. 2011. Impaired arpeggio movement in skilled reaching by rubrospinal tract lesions in the rat: a behavioral/anatomical fractionation. J Neurotrauma. 28:2439–2451.

Morris R, Vallester KK, Newton SS, Kearsley AP, Whishaw IQ. 2015. The differential contributions of the parvocellular and the magnocellular subdivisions of the red nucleus to skilled reaching in the rat. Neuroscience. 295:48–57.

Morris R, Whishaw IQ. 2016. A proposal for a rat model of spinal cord injury featuring the rubrospinal tract and its contributions to locomotion and skilled hand movement. Front Neurosci. 10:5.

Nielson JL, Sears-Kraxberger I, Strong MK, Wong JK, Willenberg R, Steward O. 2010. Unexpected survival of neurons of origin of the pyramidal tract after spinal cord injury. J Neurosci. 30: 11516–11528.

Nielson JL, Strong MK, Steward O. 2011. A reassessment of whether cortical motor neurons die following spinal cord injury. J Comp Neurol. 519:2852–2869.

Oudega M, Perez MA. 2012. Corticospinal reorganization after spinal cord injury. J Physiol. 590:3647–3663.

Paxinos G, Watson C. 2006. The Rat Brain in Stereotaxic Coordinates. Amsterdam: Elsevier Academic Press.

Pettersson LG, Alstermark B, Blagovechtchenski E, Isa T, Sasaski S. 2007. Skilled digit movements in feline and primate–recovery after selective spinal cord lesions. Acta Physiol (Oxf). 189:141–154.

Raineteau O, Fouad K, Bareyre FM, Schwab ME. 2002. Reorganization of descending motor tracts in the rat spinal cord. Eur J Neurosci. 16:1761–1771.

Raineteau O, Fouad K, Noth P, Thallmair M, Schwab ME. 2001. Functional switch between motor tracts in the presence of the mAb IN-1 in the adult rat. Proc Natl Acad Sci U S A. 98: 6929–6934.

Ramic M, Emerick AJ, Bollnow MR, O'Brien TE, Tsai SY, Kartje GL. 2006. Axonal plasticity is associated with motor recovery following amphetamine treatment combined with rehabilitation after brain injury in the adult rat. Brain Res. 1111:176–186.

Sacrey LA, Alaverdashvili M, Whishaw IQ. 2009. Similar hand shaping in reaching-for-food (skilled reaching) in rats and humans provides evidence of homology in release, collection, and manipulation movements. Behav Brain Res. 204:153–161.

Schubring-Giese M, Molina-Luna K, Hertler B, Buitrago MM, Hanley DF, Luft AR. 2007. Speed of motor re-learning after experimental stroke depends on prior skill. Exp Brain Res. 181:359–365.

Siegel CS, Fink KL, Strittmatter SM, Cafferty WB. 2015. Plasticity of intact rubral projections mediates spontaneous recovery of function after corticospinal tract injury. J Neurosci. 35: 1443–1457.

Starkey ML, Barritt AW, Yip PK, Davies M, Hamers FTP, McMahon SB, Bradbury EJ. 2005. Assessing behavioural function following a pyramidotomy lesion of the corticospinal tract in adult mice. Exp Neurol. 195:524–539.

Starkey ML, Bleul C, Maier IC, Schwab ME. 2011. Rehabilitative training following unilateral pyramidotomy in adult rats improves forelimb function in a non-task-specific way. Exp Neurol. 232:81–89.

Starkey ML, Schwab ME. 2012. Anti-Nogo-A and training: can one plus one equal three? Exp Neurol. 235:53–61.

Thallmair M, Metz GA, Z'Graggen WJ, Raineteau O, Kartje GL, Schwab ME. 1998. Neurite growth inhibitors restrict plasticity and functional recovery following corticospinal tract lesions. Nat Neurosci. 1:124–131.

Urban DJ, Roth BL. 2015. DREADDs (designer receptors exclusively activated by designer drugs): chemogenetic tools with therapeutic utility. Annu Rev Pharmacol Toxicol. 55: 399–417.

Wahl AS, Omlor W, Rubio JC, Chen JL, Zheng H, Schroter A, Gullo M, Weinmann O, Kobayashi K, Helmchen F, et al. 2014. Neuronal repair. Asynchronous therapy restores motor control by rewiring of the rat corticospinal tract after stroke. Science. 344:1250–1255.

Weidner N, Ner A, Salimi N, Tuszynski MH. 2001. Spontaneous corticospinal axonal plasticity and functional recovery after adult central nervous system injury. Proc Natl Acad Sci U S A. 98:3513–3518.

Whishaw IQ, Gorny B, Sarna J. 1998. Paw and limb use in skilled and spontaneous reaching after pyramidal tract, red nucleus and combined lesions in the rat: behavioral and anatomical dissociations. Behav Brain Res. 93:167–183.

Whishaw IQ, Pellis SM, Gorny B, Kolb B, Tetzlaff W. 1993. Proximal and distal impairments in rat forelimb use in reaching follow unilateral pyramidal tract lesions. Behav Brain Res. 56:59–76.

Whishaw IQ, Pellis SM, Gorny BP. 1992a. Skilled reaching in rats and humans: evidence for parallel development or homology. Behav Brain Res. 47:59–70.

Whishaw IQ, Pellis SM, Pellis VC. 1992b. A behavioral study of the contributions of cells and fibers of passage in the red nucleus of the rat to postural righting, skilled movements, and learning. Behav Brain Res. 52:29–44.

Whishaw IQ, Piecharka DM, Drever FR. 2003. Complete and partial lesions of the pyramidal tract in the rat affect qualitative measures of skilled movements: impairment in fixations as a model for clumsy behavior. Neural Plast. 10:77–92.

Whishaw IQ, Tomie JA, Ladowsky RL. 1990. Red nucleus lesions do not affect limb preference or use, but exacerbate the effects of motor cortex lesions on grasping in the rat. Behav Brain Res. 40:131–144.

Z'Graggen WJ, Metz GA, Kartje GL, Thallmair M, Schwab ME. 1998. Functional recovery and enhanced corticofugal plasticity after unilateral pyramidal tract lesion and blockade of myelin-associated neurite growth inhibitors in adult rats. J Neurosci. 18:4744–4757.

Zorner B, Bachmann LC, Filli L, Kapitza S, Gullo M, Bolliger M, Starkey ML, Rothlisberger M, Gonzenbach RR, Schwab ME. 2014. Chasing central nervous system plasticity: the brainstem's contribution to locomotor recovery in rats with spinal cord injury. Brain. 137:1716–1732.